

Numerical Study of Electro-osmotic Consolidation Effect on Pipe-Soil Interaction.

Hakuri Nwen Joshua* and Fuat Kara

School of Water, Energy and Environment, Energy Theme, Cranfield University, UK

Abstract

Subsea pipelines are laid directly on seabed with further constraining measures to stabilise it against adverse effect of axial walking, upheaval buckling and lateral buckling. Costly mitigating measures are being employed and the need for further investigation to explore more option is considered. Stability of soil depends on the soil strength. Increasing the soil strength has been identified as a possible mitigation against pipeline displacement. Electro-osmotic consolidation process is currently being employed to increase soil strength around offshore and onshore structures, but the effect on pipe-soil interaction has not been fully investigated. This aspect received no attention on numerical model or detail experiment in this regard. The present study numerically investigates the effect of pipe-soil interaction using capabilities of commercial ABAQUS finite element software tool on both Electro-Kinetic (EK) treated and untreated soil to determine their behaviours. Results from this study when compared with non-EK treated soil, indicates remarkable developments, as the force required to displace pipeline increases significantly due to EK treatment.

KEYWORDS: Displacement, Consolidation, Pore pressure, Effective Stress, Finite element, Electro-osmosis Electro-kinetic, Electrodes.

NOTATIONS

A	Surface area (m^2)	u	Pore water pressure (Pa)
A_c	Area of contact	v	Velocity (m/s)
b	Body force vector (N)	v^s	Soil particle velocity (m/s)
C_p	Electrical capacitance per unit volume	\bar{v}	Relative velocity (m/s)
C_v	Soil coefficient of consolidation	V	Vertical load (N/m)
D	Diameter	x	Particle position (m)
F	Force (N)	X	Particle reference configuration
F_e	Effective axial force (N)	z	Elevation (m)
F_w	Axial force on pipe wall (N)	α	Coefficient of thermal expansion
L	Length (m)	α'	Adhesion factor
k_{eo}	Electro-osmotic permeability m^2/Vs	β	intermittent power supply
k_w	Hydraulic conductivity m/s	σ	Total Cauchy stress (Pa)
k_{se}	Electrical conductivity (S/m)	σ'	Effective Cauchy stress (Pa)
j	Electrical current density (A/m^2)	φ	Mapping function
L_0	Original length (m)	π	Moving particle phase
p_e	External pressure (Pa)	γ_w	Soil unit weight
p_i	Internal pressure (Pa)	ϕ	Electric potential (V)
s	Solid particle	θ	Temperature ($^{\circ}C$)
S_u	Undrained shear strength, (Pa)	I	Electrical current (A)
t	Time (s)	ν	Poisson ratio

1 Introduction

Material strength relates to the greatest stress it can withstand. Low strength of soil may lead to collapse of structures resting on it. The ability of a pipeline to overcome axial displacement depends on the strength of soil in contact with the pipeline. Deepwater consists mostly of very soft clay with high water content, low shear strength and high compressibility [1,2]. Reduction in the moisture content in the soil due to the release of pore water pressure increases the soil undrained shear strength. Shear box testing gives credence to this process of increasing axial resistance due to cyclic hardening of soil [3]. Another concept at improving soil shear strength is Electro-Kinetic (EK) process. This concept is similar to the above in such that all involves a decrease in pore water pressure from the soil and one important advantage is that the time taking for soil to consolidate is highly reduced. This method find it application at increasing soil-bearing capacity of onshore and offshore structures. As obtained in the other processes, the EK process helps to reduce the pore water pressure in the soil. Applying the EK method to a pipeline which is susceptible to buckling and walking has been carried out experimentally by Eton [4]. The phases involve electro-osmotic consolidation process followed by stress displacement analysis of the pipe-soil interaction. Results from the experiment indicates remarkable developments as the soil shear strength increases significantly due to EK treatment. Numerical investigation of EK process on the pipe-soil interaction to a very soft soil has received almost no attention. The present study investigates numerically the impact in which treated soil will have on pipe-soil interaction using ABAQUS, a commercially available software package. With proper design and configuration of electrodes around the pipe, the EK approach on pipe-soil interaction will result in significant increase in soil shear strength thereby mitigating against pipeline displacement.

1.1 Electro-Osmotic Concept

Electro-osmosis process to increase the strength of soil is conducted by applying electrical voltage to electrodes. Due to voltage flow, the soil pore water pressure tends to move from the anode to cathodes as shown in Fig. 1 [5]. The electric potential applied to soil will

lead to the generation of negative pore pressure where the drainage condition is being determined by the anode and cathode of the electrode. Pore water pressure being generated lead to an increase in the effective stress of the soil with the total stress experiencing no changes and subsequently, leading to consolidation due to soil compartment [6]. The induced water flow due to ion migration can also lead to movement of other contaminant in the soil, which depends on factors such as the soil and pore water conductivity [7].

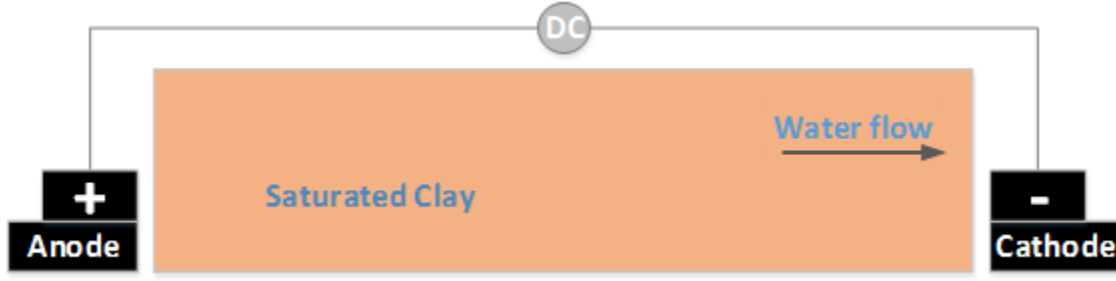


Fig. 1 Electro-kinetic phenomena: electro-osmosis (adapted from [8])

EK process found its application on both saturated and unsaturated soil. Electro-osmosis offers great benefit such that, the time taken for soil consolidation is highly reduced and surcharge loading avoided [9]. A normally consolidated soft clay has shown to be over-consolidated when treated and the over-consolidated ratio can be achieved in the range of about 1.2 and 1.7 while the soil shear strength can witness an increase of about 100% to 200% [10]. As stated by Al-Hamdan and Reddy [10], the undrained soil shear strength increases further after the EK treatment mainly due to the soil hardening as a result of ionic diffusion and is permanent. Considerable increase in the soil shear strength around the anodes [11] has been observed. A recent approach by Eton [4] of which the soil modification was applied to pipelines on soft clay soil indicated a considerable improvement in the soil strength.

A three-dimensional (3-D) model was analysed by Micic, Shang and Lo [12] considering the material behaviours and boundary conditions. HU and WU [13] also presented a two-dimensional (2-D) and 3-D numerical analyses of the field test conducted by Bjerrum, Moum and Eide [14]. Yuan, Hicks and Jommi [15] also conducted a numerical study based on the field test reported by Bjerrum, Moum and Eide [14] in 2-D considering large strain and constitutive elasto-plastic behaviour of the soil. Yuan and Hicks [16] presented numerical analyses of a multi-dimensional model based on field data given by Burnotte, Lefebvre and Grondin [17]. The complex geometry with multiple electrodes and intermittent current were determined. Other conditions such as the material nonlinearity and the soil elasto-plastic behaviour were considered.

1.1.1 Constitutive Equations

As given by Yuan and Hicks [16] mass conservation of water is given by the equation:

$$\nabla \cdot (\mathbf{v}^s + \bar{\mathbf{v}}) = 0 \quad (1)$$

where the soil particle velocity is given as \mathbf{v}^s and the water filtration velocity relative to the soil skeleton is $\bar{\mathbf{v}}$. The fluid flow due to electrical and hydraulic gradient can be coupled to give a total flow [18–20]:

$$\bar{\mathbf{v}} = -\frac{k_w}{\gamma_w} (\nabla p + \gamma_w \mathbf{z}) - k_{eo} \nabla \phi \quad (2)$$

where the hydraulic conductivity, soil unit weight and the elevation is given by k_w , γ_w and z respectively, the electro-osmotic permeability is k_{eo} and electric potential given as ϕ .

Assuming a charge conservation with steady state current, the electrical field governing equation is given as Yuan and Hicks [16]:

$$-\nabla \cdot \mathbf{j} = C_p \frac{\partial \phi}{\partial t} \quad (3)$$

where the electrical current flux is given as \mathbf{j} , the electrical capacitance per unit volume as, C_p . Assuming C_p is negligible and based on ohms law, the electrical flow can be represented as:

$$\mathbf{j} = -k_{\sigma e} \nabla \phi \quad (4)$$

where the electrical conductivity is $k_{\sigma e}$.

For a constant hydraulic pressure, the excess pore water pressure u_e can be obtained from equation [18–20]:

$$\nabla^2 u_e + \frac{k_{eo}}{k_h} \gamma_w \nabla^2 \phi = -\frac{1}{c_h} \frac{\partial u_e}{\partial t} \quad (5)$$

$$\text{where, } c_h = \frac{k_h}{m_v \gamma_w} \quad (6)$$

c_h is the coefficient of consolidation.

The increase in the soil effective stress σ' due to the reduction in pore water pressure u given by:

$$\Delta \sigma' = -\Delta u \quad (7)$$

The soil compressibility and strength depends on the effective stress within the soil particles. Total pressure within the soil consist of various component within the soil and is considered to be the same at every point under equilibrium conditions [21]. The flow of pore water can occur within the soil if a difference is created at certain points. Total pore pressure consist of many components amongst which are the hydrostatic pressure and the osmotic pressure [21]. The hydrostatic pressure occurs due to incomplete saturation and externally applied load. The osmotic pressure usually occurs due to difference in ionic concentration within the soil as previously described by Mitchell and Soga [8] in Fig. 1, pore water flows from higher concentration to lower concentration. Osmotic effect has been one of the main cause of negative pore pressure and could take place in both saturated and partially saturated soil [21].

1.1.2 Energy Consumption

The intensity of power being applied will also affect the corrosion rate of the electrodes. The cost of electrodes and power consumption will therefore, play an important role in this case. Two major problems encountered with the EK process were the corrosion of the anode and high conductivity of marine clay requiring high power supply, these challenges however, can be addressed in part by applying intermittent current [10]. Details on this electro-osmotic process is covered in [10,16]. Distribution of voltage between electrodes as observed by Lo, Micic and Shang [22] is approximately linear with no significant drop however, the conductivity of the soil experiences considerable decrease leading to drop in current flow at the soil-electrode-water interface [22]. Most studies assumed constant electrical and mechanical properties during electro-osmosis process. Some report were also made in [20,23,24] on the possibility of increasing the current density by polarity reversal. However, this aspect was not considered in this study. Equations defining the electrical properties in the EK treatment are giving in [10] as outlined below.

The power consumption rate:

$$P = j \times \beta \times \Delta \phi / \Delta L \quad (8)$$

where the current density

$$j = \frac{I}{A} \text{ (A/m}^2\text{)} \quad (9)$$

$$\beta = \frac{\text{power ON time}}{\text{power ON+OFF time}} \quad (10)$$

(i.e. for the intermittent power supply) and $\frac{\Delta \phi}{\Delta L}$ (V/m) is the voltage gradient.

1.1.3 Flow Equations and Similarities

Provided the rate of flow is linearly related to the gradient and all properties and boundary conditions are well defined, the flow from one of the equations can be used to solve related problems [8]. Laws relating to heat, electrical, chemical and hydraulic flows are shown in Table 1.

Table 1 Similarities of flows conduction in porous media (adapted from [8])

	Fluid	Heat	Electrical	Chemical
Potential	Total heat h (m)	Temperature θ ($^{\circ}\text{C}$)	Voltage ϕ (volts)	Concentration c or Chemical Potential μ (mol/m^3)
Storage	Fluid volume V (m^3/m^3)	Thermal energy u (J/m^3)	Charge Q (Coulomb)	Total mass per unit total volume, m (mol/m^3)
Conductivity	Hydraulic conductivity k_h (m/s)	Thermal conductivity k_t $\text{W}/\text{m}/^{\circ}\text{C}$	Electrical conductivity σ (Siemens/m)	Diffusion coefficient D (m^2/s)
Flow	q_h (m^3/s)	q_t (J/s)	Current I (amp)	j_D (mol/s)
Gradient	$i_h = -\frac{\partial h}{\partial x}$ (m/m)	$i_t = -\frac{\partial \theta}{\partial x}$ ($^{\circ}\text{C}/\text{m}^3$)	$i_e = \frac{\partial \phi}{\partial x}$ (V/m)	$i_h = \frac{\partial h}{\partial x}$ (mol/m^4)
Conduction	Darcy's law $q_h = -k_h \frac{\partial h}{\partial x} A$	Fourier's law $q_t = -k_t \frac{\partial \theta}{\partial x} A$	Ohm's law $I = -\sigma_e \frac{\partial \phi}{\partial x} A = V/R$	Fick's law $J_D = -D \frac{\partial c}{\partial x} A$
Continuity	$\frac{\partial V}{\partial t} + \nabla \left(\frac{q_h}{A} \right) = 0$	$\frac{\partial u}{\partial t} + \nabla \left(\frac{q_t}{A} \right) = 0$	$\frac{\partial Q}{\partial t} + \nabla \left(\frac{I}{A} \right) = 0$	$\frac{\partial (m)}{\partial t} + \nabla J_D = 0$
Steady state	$\nabla^2 q_h = 0$	$\nabla^2 q_t = 0$	$\nabla^2 I = 0$	$\nabla^2 J_D = 0$

1.1.4 Pipe Embedment

Finite element approach at determining the vertical penetration of pipeline has been conducted by Merifield, White and Randolph [25] with pipeline placed at a predetermined depth known as wished in pipe (WIP) [26] and with a pipeline allowed to penetrate based on its own weight or operational load known as pushed in pipe (PIP) described in Fig. 2. It was discovered that higher penetration force is required to displace the soil for the PIP than the WIP due to heave formation around the pipe surface [27]. Pipeline laid on undrained clay soil will be sustained by the soil pore water pressure. A gradual dissipation of the pore pressure over time will account for the effective stress, and in this case, the soil skeleton will be involved. Further embedment of pipeline with pore water dissipation leads to local consolidation at the pipe invert surface. This takes place over a period and governs the drained or undrained behaviour of a pipeline. Better understanding of the pore pressure behaviour and the effective stress is vital in accounting for the pipeline initial embedment.

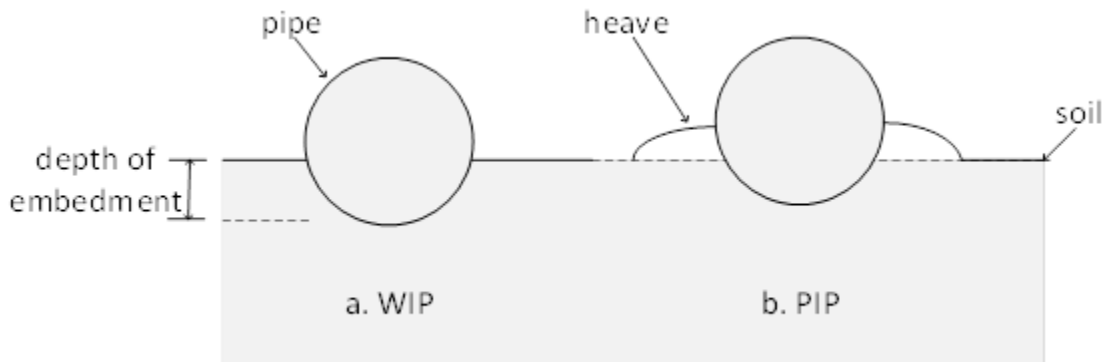


Fig. 2 a. Wished in Pipe, (WIP) b. Push in Pipe, (PIP)

The pore fluid analysis can be determine in terms of total or excess pore water. The total pore pressure analysis considered the gravity loading to define the load on the soil while the excess pore pressure considered both the gravity and distributed body load due to pressure. The relationship defining the undrained vertical displacement of pipeline with load is represented by the parameters shown below [28].

$$V = f(E, S_w, D, z, v, \gamma', C_i) \quad (11)$$

where V is the vertical load per unit length; E , is the young modulus; S_u , the soil undrained shear strength; D , pipe diameter; z , depth of embedment; ν , soil Poisson ratio; and γ' soil effective unit weight; C_i , adhesion of pipe-soil. The embedment of the pipe into the soil can be determine using the non-dimensional function.

$$\frac{V}{DS_u} = \phi' \left(\frac{E}{S_u}, \frac{z}{D}, \nu, \frac{C_i}{S_u}, \frac{\gamma' D}{S_u} \right) \quad (12)$$

The vertical reaction law accounting for both the laying and dynamic installation effect for determining embedment of pipeline is giving in [29–31]. Pipe embedment shows a non-linear elastic response, the coupling of axial resistance with pipe embedment will give a more realistic result and pipe embedment to a large extent depends on the area of contact [32,33].

The interaction of the pipe-soil in deepwater is usually in an undrained or partially undrained condition due to the existence of excess pore pressure [1]. This depends on the consolidation coefficient, length of drainage path, level of stress subjected to the soil and the displacement rate in the axial direction. Deepwater soft clay soil is characterized by undrained shear strength of approximately zero at the mudline, with the strength gradient extending from 5-15kPa/m. The bearing pressure ranges between 1-10kPa [1]. Determination of the drained and undrained condition of soil are given the equations below [34].

$$\text{Fully drained condition, } \frac{vD}{C_v} < 1 \quad (13)$$

$$\text{Fully undrained condition, } \frac{vD}{C_v} > 20 \quad (14)$$

where v , pile velocity; D , diameter and C_v , soil coefficient of consolidation.

2 Numerical Model Development

This study uses the ABAQUS 2016 to demonstrate its capabilities in solving EK problems. Three phases were developed for this study: the first phase is the verification of the different flow process in ABAQUS. This help to confirm the capability of any of the flow process to mimic electrical flow due to their similarities as shown in Table 1.

Table 1. The second phase is the verification of the coupled temperature–pore pressure element to mimic coupled electrical-pore pressure for the electro-osmotic consolidation of the clay soil. The third phase consist of the electro-osmotic consolidation and dynamic pipe-soil interaction analyses to confirm the effect of EK treated soil on pipe-soil interaction. The resistance developed due to pipe-soil interaction from EK and non-EK treated soil are then measured and compared.

2.1 Models Assumptions

Assumptions made for the analyses are:

1. The electrodes: anode and cathodes are of the same materials.
2. Electrical potential at the cathodes is zero.
3. There is constant electrical conductivity at the electrodes, soil and water during the analyses
4. There is zero electrical potential at the soil/water surfaces.
5. Voltage gradient is directly proportional to the fluid velocity
6. Effect of electrochemical reaction is not considered.
7. Uniform pore pressure is assumed in the soil

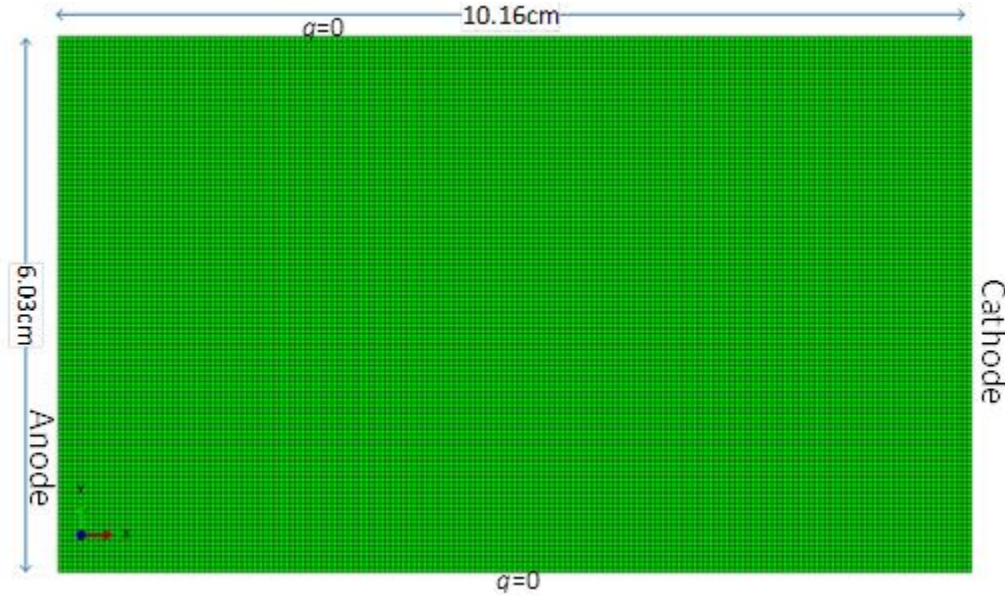
2.2 PHASE 1: ABAQUS Heat Transfer, Electrical and Chemical Flow Verification

The first step in verification of procedure being adopted is the determination of ABAQUS heat transfer capability to mimic electrical flow due to similarities shown in Table 1. Numerical analysis was conducted based on parameters obtained from Hansen and Saouma [35] on steel corrosion and concrete cracking as shown in Table 2. The geometry consist of concrete dimension 10.16 x 6.03cm and electrodes dimension of 6.03 x 0.16cm as shown in Fig. 3. Current density, q at the model surface were set at zero. The boundary at the anode was set with voltage of 0.440V and at the cathode with -0.417V. The concrete served as the electrolyte while the potential at the anode and cathode represented the mass concentration (for an electrochemical reaction).

A two dimensional (2-D) analyses: heat transfer, mass diffusion and electrical flow procedure in ABAQUS were considered for comparison. The heat transfer and mass diffusion flow process was modelled with DC2D4 (a 4-node linear heat transfer quadrilateral) element. The electrical flow process is modelled with DC2D4E (a 4-node linear coupled thermal-electrical quadrilateral) element. Coupled temperature-displacement procedure is modelled with CPE4RT (a 4-node plane strain thermally coupled quadrilateral, bilinear displacement and temperature, reduced integration, hourglass control).

Table 2 Flow process validation parameter [35]

Properties	Values
Resistivity of concrete	5000 ohm-cm
Potential at anode	0.440V
Potential at cathode	-0.417V
Analysis time	Steady state

**Fig. 3 Phase-1: ABAQUS heat transfer, electrical and chemical flow verification model**

2.3 PHASE-2: ABAQUS Coupled Temperature-Pore Pressure Elements Verification

To verify the capability of coupled temperature-pore pressure element to mimic electrical-pore pressure for the EK analyses, numerical study was conducted and compared with numerical analysis conducted by Yuan and Hicks [16]. The model as shown in Fig. 4.a and b consists of 12 anodes and 12 cathodes of steel electrodes, each 5m long and 0.17m in diameter. The anodes and cathodes were arranged in four rows spaced at 3m, each of the rows consist of six anodes or six cathodes separated 2m apart. All electrodes were set at the same levels extending to depth of 14m from the top surface of the soil. The clay soil dimension consists of 49 x 20 x 20m. Water table is set at 3.1m and the pore water pressure above the water table set to zero. The vertical and bottom surface boundaries were set to be impermeable with free drainage allowed at the top vertical surface of the cathodes. Each of the cathodes has voltage of zero and voltage gradient of 0.33V/m between pairs of the electrodes (anode and cathode). Displacement is prevented in the horizontal direction and impermeable. The bottom surface boundary is fixed and impermeable with free drainage allowed at the cathodes.

Treatment time for the electro-osmosis is 50 days. Tie constraint between the electrodes and the soil is set with the electrodes being the master surface and the soil being the slave surface. The FE models for electrodes and soil are modelled with 10-nodes modified quadrilateral tetrahedron, pore pressure and temperature, hourglass control, C3D10MPT. Modified Cam clay soil model is based on parameter obtained in [16,17] shown in Table 3. Critical state line, M is 0.567, poison ratio, ν of 0.3, and pre-consolidation pressure is 120kPa, hydraulic conductivity, k_w of $1.5 \times 10^{-12} \text{ m/s}$ and electro-osmotic permeability, k_{eo} of $3.5 \times 10^{-9} \text{ m}^2/\text{V.s}$. The model assembly is described in Fig. 5, further details on the arrangement are given in [16,17].

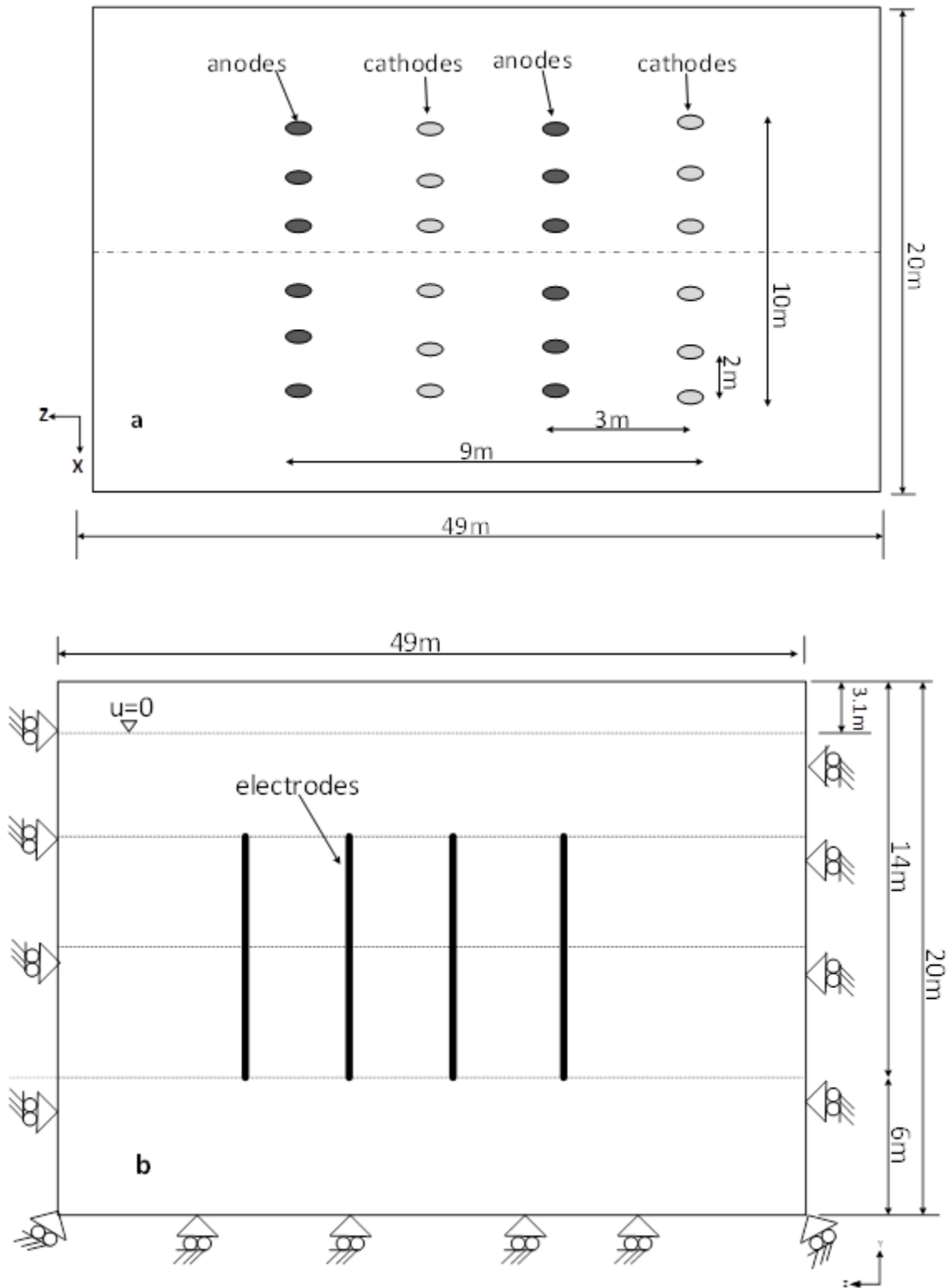


Fig. 4 Phase-2: Electro-osmotic consolidation model geometry description: (a) plan view (b) vertical side view

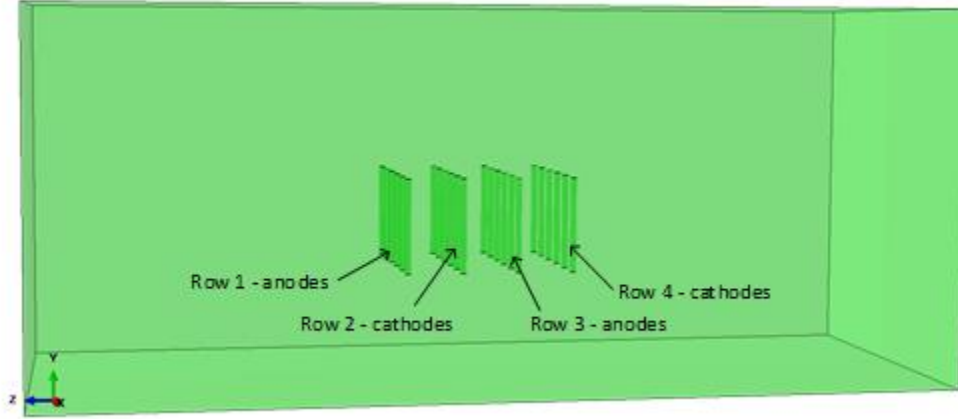


Fig. 5 Phase-2: Model Assembly

Table 3 Soft clay soil parameters [16,17]

Properties	Values
Hydraulic conductivity, k_h	$1.5 \times 10^{-12} m/s$
Electro-osmotic permeability, k_{eo}	$3.5 \times 10^{-9} m^2/V.s$
Electric conductivity, $k_{\sigma e}$	$1.0 S/m$
Virgin consolidation line, λ	0.316
Recompression/swelling line κ	0.045
Slope of critical state line	0.567
Poisson's ratio ν	0.3
Coefficient of earth pressure at rest, K_0	1.0*
Unit weight of soil, γ	$16.4 kN/m^3$

2.4 PHASE 3: EK Pipe-Soil Interaction Model

This section explains the procedures followed in the analyses. Pipe-soil behaviour with and without EK treatment were considered. Three stages are involved in the simulation: geostatic, electro-osmosis (consolidation), and dynamic analysis. The measurement and comparison of the resistance developed between the EK and non-EK treated soils were determined. To ensure stress equilibrium of the soil, the first step in the analyses is the geostatic step. In this step, ABAQUS assumed a displacement of zero and where a non-zero is obtained, this value is neglected. The second step is the soil consolidation (EK) step in which the procedure “SOIL” in ABAQUS is adopted. The third step is adopted using the dynamic implicit procedure to determine resistance generated due to pipeline displacement before and after the EK treatment of the soil.

2.4.1 Electro-Osmotic Consolidation Modelling

ABAQUS software tool has no direct capabilities to support electro-osmotic process, however, based on the relationship with different flow processes as given in phase one and two, the mass diffusion or heat transfer analysis procedure can be used to mimic the electrical flow [35]. The governing law relating the flow process: fluid, electrical, chemical and heat transfer are shown in Table 1. Thermal conductivity in the heat transfer procedure in ABAQUS tool is based on the Fourier law shown in Table 1. The conductivity k_t can be isotropic, anisotropic orthotropic [36]. Based on relationships with the different flow process, couple temperature-pore pressure element in ABAQUS software package is adopted. Tie interaction constrain between the soil/water and electrodes is adopted to ensure electrical contact. Initial time increment for the electro-osmotic model is determined from Eqn. 15 [37,38].

$$\Delta t_{initial} = \frac{h^2 \gamma_w}{6E'k} \quad (15)$$

where h , the average dimension of element k , soil permeability; and E , soil effective young modulus. To account for non-linearity in the geometry the NLGEOM parameter is set on, through all analyses.

Selecting the approximate global size of elements is not straight forward, however the optimal number of elements was determined by considering all cases ranging from coarse to fine mesh in the mesh refinement analyses. Convergence test is one of the effective means being considered for determining the element size adopted. In the convergence test, the error resulting from the calculated values tend to converge to zero as the number of element increases. In all cases from this study, the slave surface is finer than the master surface to avoid substantial penetration into the master surface for more accurate results. The test was conducted with the pipe, soil, electrodes and rings having element size of 0.04m, 0.033m, 0.035m and 0.0025m respectively.

2.4.1.1 Model Schematic Overview

The WIP method as described in Fig. 2 is adopted in this study mainly to allow for electrical contact between the soil and anodes. The disadvantage of this method is the absence of initial pore water pressure generated during the pipe penetration as reported in [39,40], which is encountered in PIP. The pore water pressure generated is due to further embedment from the predefined WIP depth. This relatively will account for a lower penetration force to be observed than when PIP method is adopted. However, this study compares the non-EK and EK process under same conditions with regard to the WIP method to account for the soil settlement and the related strength developed on pipe-soil interactions. Unloading and reloading analyses of the pipe was not considered.

Layout of the electrodes for the electro-osmosis analysis is shown in Fig. 6, the electrodes are equal in length to the pipe, installed together and separated by supporting rings shown in Fig. 10. The anodes are embedded in the soil inclined at an angle 10° . The same applied to the cathodes except they are embedded in the water. The pore water assume to flows in the vertical direction and distance x between the anodes and cathodes create the potential gradient $i_e = \frac{\partial \phi}{\partial x}$ as given previously in Table 1. Zero potential assumed at the soil surface allows the electrical flow to be notice in all direction. However, as derived from Rittirong and Shang [41] the thickness W and width of the soil (soil/water) L is far greater than the distance between anodes and cathodes x (*i. e* $W, L \gg x$), the flow can be considered in two dimensions, x-y plane.

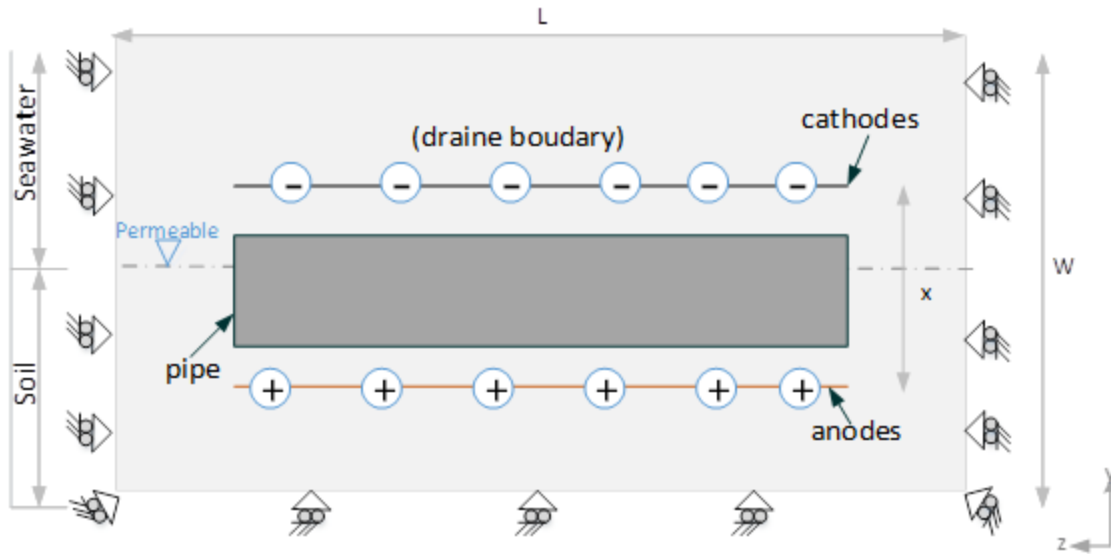


Fig. 6 Phase-3: Schematic model configuration of electro-osmotic process

Below is a schematic of the models arrangements for the pipe-soil interaction, conducted with regards to the pipe vertical penetration in Fig. 7, the pipe axial displacement in Fig. 8, and the pipe lateral displacement in Fig. 9. These represent all test conducted for both the electro-osmosis and dynamic analyses in Phase-3 of this study. These were detailed in next sections below.

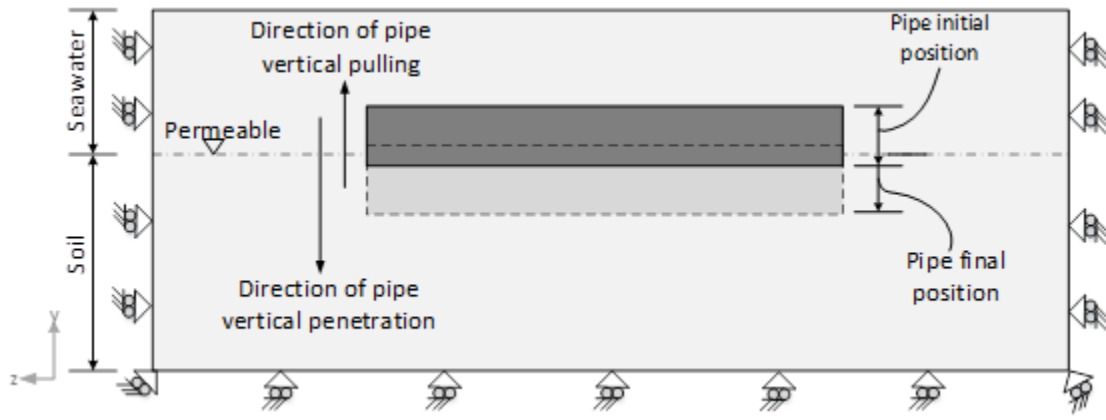


Fig. 7 Phase-3: Schematic Side view of model position for pipe vertical penetration test

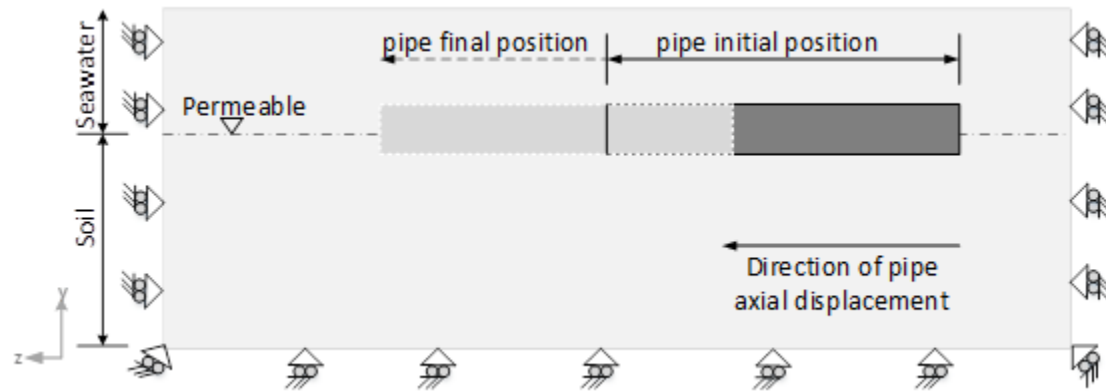


Fig. 8 Phase-3: Schematic of model position for pipe axial displacement test

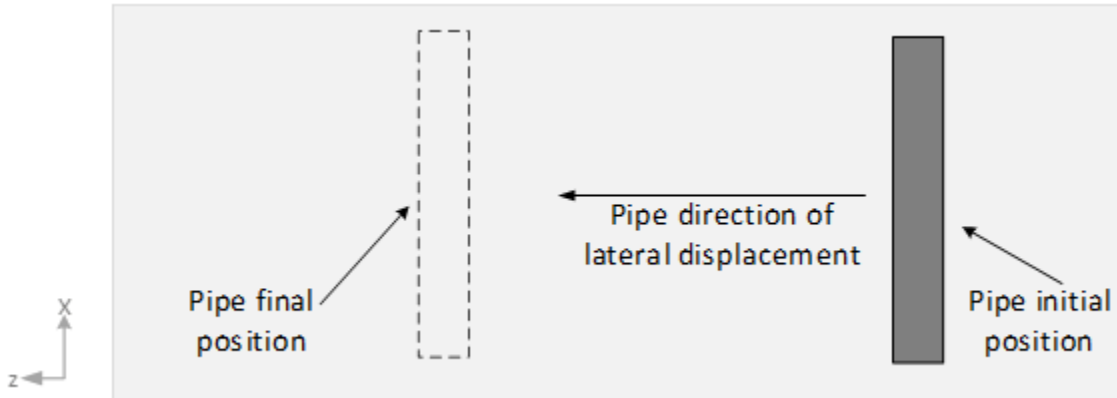


Fig. 9 Phase-3: Schematic Plan view of model position for pipe lateral displacement test

2.4.1.2 Boundary Conditions

The electrodes boundary conditions are assigned with temperature $\theta = \theta(x, t)$ to mimic the voltage $\phi = \phi(x, t)$. The model pipeline is assumed to be straight with the end boundary conditions assumed unconstrained. The vertical boundaries beside soil surfaces are set to allow for displacement and permeable in the vertical direction with no displacement in the horizontal surfaces. Bottom surface of the soil is fixed and impermeable. The water level is set at the top surface of the soil and permeable with zero pore water pressure assumed. Other condition are defined in the test series in subsequent sections.

2.4.1.3 Electrode Materials Consideration

Electrodes material selection are based on their availability, cost and suitability for EK treatment. Materials often used includes copper, mild steel and aluminium with consideration to their durability, conductivity, and chemical properties. EK soil treatment is related to the intensity of the electrical field, which depends on the layout of the electrode in consideration. Hence, the appropriate selection of the electrode materials will determine the optimum performance in service. In field application the cathode normally acts as the drain, however due to its application in seawater, the seabed surface will act as the drain. The seawater has higher conductivity than clay and as stated by Eton [4], the seawater resistivity can be neglected. The seawater in this case is treated as the cathode, which give the reason for adopting less numbers of cathodes (and in this case two) when compared with numbers of anodes.

This study does not consider different types of electrodes materials as only the iron electrodes are employed. Eton [4] Indicates that iron material is more effective for a partially embedded material in the soil. Iron material also has its limitations with regards to its faster rate of corrosion in aggressive saline environment. Studies have shown that the electrode type is significant in the EK process, this depends on the material conductivity and its resilience during the treatment time [42–44]. Further details on the material properties are given in subsequent sections for each of the model series.

2.4.1.4 Model Properties

Materials selected are based on suitability, known physical and chemical properties and the ability to be compared with known test that have been conducted. Polwhite E grade kaolin a common constituent of many actual clay soils with suitable geotechnical and chemical properties will be considered based on experiment by Eton [4]. Its main constituents are hydrous aluminium silicate clay mineral kaolinite. The pipe-soil model is described in Table 4 and the electro-osmotic properties in Table 5. The soil dimension of 2m x 0.9m x 0.7m represent soil/water with water depth of 0.3m and soil depth of 0.4m. The seabed soil is considered uniformly homogenous. Kaolin clay is used, the soil is assumed to be in a normally consolidated state for a saturated soil with 70% water content and void ratio of 1.5. Cam clay model is used in the test [37,45]. Anodes and cathodes are of the same iron material. Steel pipe with the mechanical behaviour assumed to be linear elastic. The pipe is WIP at a depth of 0.5D for the vertical, axial and lateral pipe-soil interaction.

Table 4 Pipe/Soil Model [4]

Parameters		Values
Soil	length	2m
	wide	0.9m
	depth	0.7m
Pipe	length	0.8m
	diameter	0.13m
Electrodes	length	0.8m
	diameter	0.0076m
Supporting rings	outside diameter	0.17m
	inside diameter	0.13m
	thickness	0.03m
	holes diameter	0.0076m
	angle between holes	10°

Table 5 Electro-osmotic/Cam Clay model parameters

PARAMETERS		MATERIALS	VALUES	UNITS
Electrical Conductivity $k_{\sigma e}$	[8,46,47]	Soil	1.0	S/m
		Seawater	4.8	S/m
		Iron electrode	1.0×10^7	S/m
		Soil	1×10^{-9}	m/s
		Soil	5.5×10^{-9}	$m^2/V.s$
		Soil	70	%
Hydraulic conductivity k_h	[37]	Soil	1.5	
Electro-osmotic conductivity k_{eo}		Soil	0.4	
Saturation S		Soil	0.115	
Void ratio e_o		Soil	1	
Virgin consolidation line, λ		Soil	1	
Recompression/swelling line k		Soil	1	
Slope of Critical state line M		Soil	1	
Coefficient of earth pressure at rest, k_o		Soil	1	
Wet yield surface size		Soil	0.333	
Poisson ratio ν		Soil	1.8×10^6	MPa
Young Modulus E	Anodes	Soil	1121	kg/m^3
Dry density γ		Soil	0	
Electrical potential (ϕ)	Cathodes		2.5-25	V
			0	
Time (t)	Steady State and Transient			s

The FE models for electrodes, support rings, and soil/water are modelled with 10-nodes modified quadrilateral tetrahedron, pore pressure and temperature, hourglass control, C3D10MPT and the pipe is modelled with 6-node triangular thin shell element STRI65 [36]. Two supporting rings, two cathodes and the six anodes were adopted using the critical state model. Fig. 10 described the pipe-electrode assembly. The axial pipe-soil model arrangement is shown in Fig. 11.

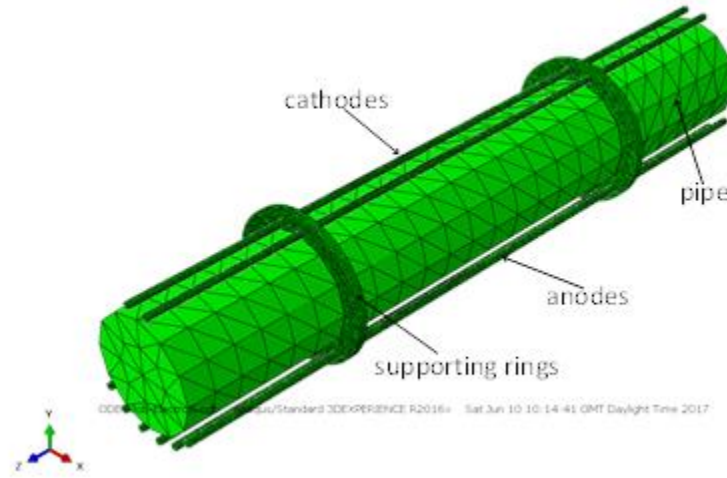


Fig. 10 Phase-3: Pipe-electrodes assembly

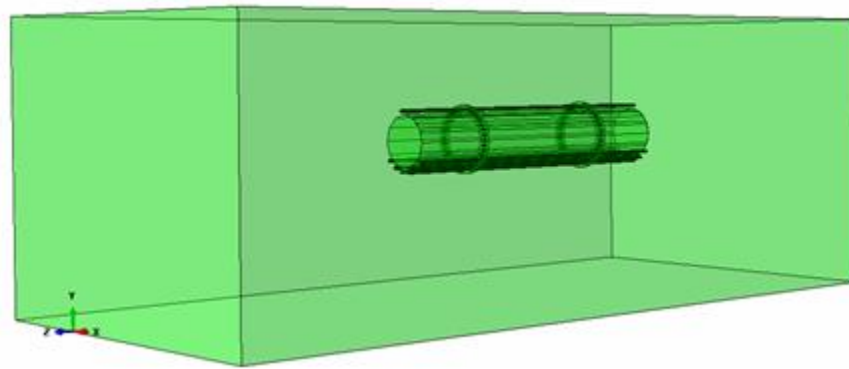


Fig. 11 Phase-3: FE axial pipe-soil interaction model

EK pipe-soil interaction analyses in vertical, axial, and lateral directions were conducted for both steady state and transient analyses. Time duration of 6, 12, and 24 hours were considered for the electro-osmotic process, subjecting the soil to electrical voltages between 2.5–25V.

2.4.2 Dynamic Modelling

Both dynamic EK and non-EK analyses were conducted and results obtained between the two are compared. The dynamic non-EK analyses are conducted without the effect of electrical flow while the EK is conducted to determine the effect of electro-osmotic consolidation on the pipe-soil interaction. Properties for this test model are the same with electro-osmotic test model as given in Table 4 and Table 5. The 3D dynamic implicit procedure is used for the dynamic analyses of the pipe-soil interaction. The contact properties have tangential behaviour with coefficient of friction set to rough ($\mu = \infty$), and normal behaviour set to hard contact. Surface to surface interaction set to finite sliding formulation is adopted with the pipeline and soil being the master and slave surface respectively. The vertical boundaries of the soil surface are set to allow for displacement in vertical direction only, while the bottom surface is fixed. Velocity of 0.0003m/s is applied for the vertical penetration while the axial and lateral displacement with velocity of 0.0005m/s. As given in Eqn. 14, these velocities are sufficient to cause undrained condition in the soil to occur with detailed analyses given in [29–31].

Two stages considered in the design for axial pipe-soil response are the peak (breakout resistance) and residual resistance. Initial axial movement of the pipeline or when pipeline moves after resting for some time is usually associated with peak resistance. The mobilisation resistance occurs at the peak resistance [1,2]. As noted in [1,48], pipe-soil response is nonlinear and the high initial stiffness tangent being produced increasingly reduces till the peak resistance is attained. Residual resistance accompanied with large displacement follows the breakout point of peak resistance. The residual resistance initially decreases rapidly and then slows down to a certain value. Peak friction is very significant at reducing the rate of walking leading to decrease in the anchors load. The undrained axial resistance can be determined using the Alpha approach for both the peak and residual resistance [30,32,33]:

$$F = A_c S_u \alpha \quad (16)$$

where S_u , the soil shear strength and α , the adhesion factor, A_c , the area of contact of pipeline with soil, given by the relationship:

The axial resistance of a pipeline subjected to cyclic loading is centred on the decline in the peak resistance, typical thixotropic plot [33] show that peak axial resistance is effective for a period of few months. The operational loading cycles for the pipeline is normally designed to operate for few month and shut-down for few hours or days and soil thixotropic with regard to walking verified. Understanding of the pipeline expansion mechanisms will require knowledge of the effective axial force, which is governed by the “(true) axial force on the wall of pipeline and the axial force due to fluids pressure. This is represented by the equation below[1,49]:

$$F_e = F_w + p_e A_e - p_i \cdot A_i \quad (17)$$

where, F_e is the effective axial force, F_w the axial force on pipe wall, p_e the external pressure, and p_i the internal pressure, A_e & A_i are the external and internal area of pipe respectively.

Main stages to consider in lateral buckling design are the breakout force, the suction release the residual force, and the cyclic lateral frictional force [50]. A considerable peak force is observed when a pipe is about to move and depends on the embedment level during the process. The breakout force occurs with a suction effect inform of a crack between the wall of the pipe and soil, with little effect on its further behaviour. Under very slow loading and before a fully mobilised peak force is observed, the crack is formed. The initial breakout force usually takes place very fast, with tension to certain degree developed at the pipe rear, leading to soil failure experienced at both ends of the pipe. During movement of the pipe, the peak force falls, leading to a residual lateral force, which raises and maintained at a steady state over a large displacement. Residual force controls the displacement during first loading and determine the initial buckle shape and peak bending stress of the pipe [50]. For cyclic lateral movement of the pipe, berms are formed on each side of the pipe. The berms contribute some resistance to pipe displacement and the buckle formation [50]. Many studies and design were introduced to address this challenge, this ranges from understanding the behaviour of the pipeline response to force and displacement, loading cycles, and point of failure [50]. Further details were discussed by [2,51–54].

3 ELECTRO-OSMOTIC CONSOLIDATION ASSESSMENT

Results from the electro-osmotic analyses of the pipe-soil interaction are presented in this section. The analyses involves the verifications of the flow processes and the pore-pressure elements/procedures being adopted for consolidation analyses of the soil using the ABAQUS tool. Both transient and steady state analyses with varying voltages are presented.

3.1 PHASE-1: ABAQUS Heat Transfer, Electrical and Chemical Flow Validation

To determine the capability of ABAQUS using the various flow process outlined in Table 1, analyses were conducted for each of the process. From Fig. 12, the flow process originates from the anodes to cathodes. By conduction, voltage is passed from anode to concrete and from the concrete to the cathodes. Areas embedded with anodes have the same potential of 0.440V and consequently decrease as it moves away from the anodes. Results of the different flow process indicates the same trends as shown in Fig. 12. This verify the choice of ABAQUS heat flow to mimic the electrical flow.

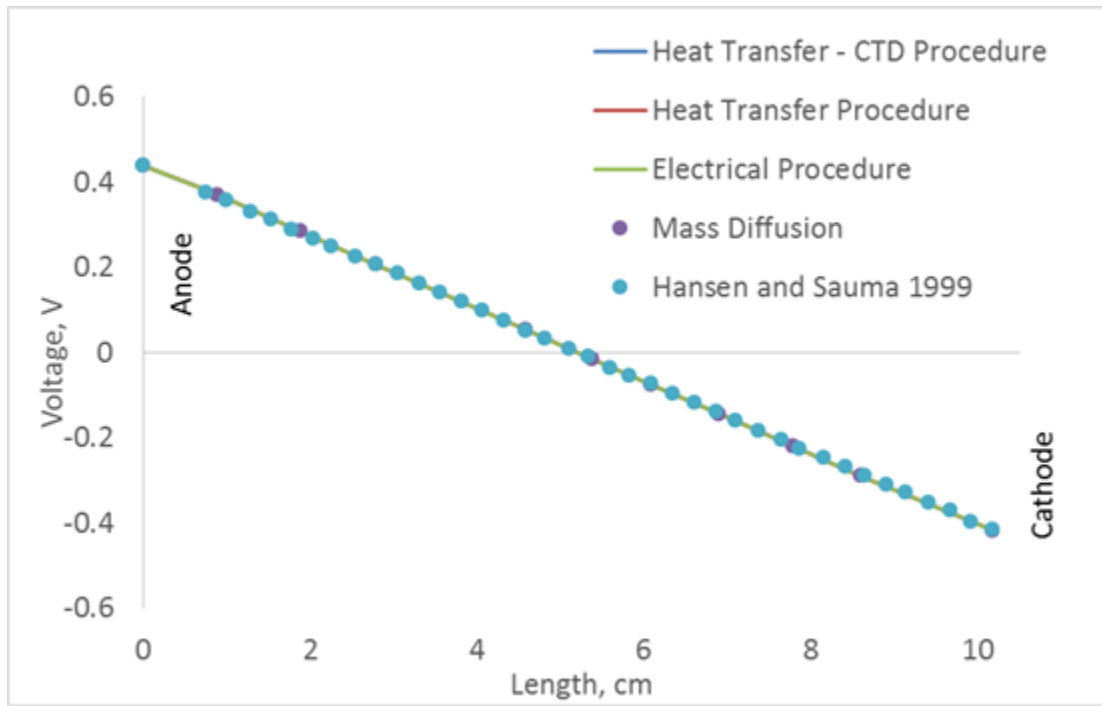


Fig. 12 Phase-1: ABAQUS flow process verification using chloride diffusion cracking of concrete

3.2 PHASE-2: ABAQUS Temperature-Pore Pressure Elements Validation

To further confirm the capacities of the coupled temperature-pore pressure procedure in ABAQUS tool to mimic coupled electrical-pore pressure, analyses were conducted and the results are shown in Fig. 13 and Fig. 14. From Fig. 14, the soil behaviour indicates higher settlement for the first 40 days of the treatment when compared with [16,17]. However, from day 40, a contrast to the analysis by Yuan and Hicks [16] is observed, the soil settlement shows a rebound. This could be attributed to less influence of the soil treatment within these periods. From the experiment, rebounds of soil settlement is due to absence of voltage, however this analysis does not consider intermittent voltage flow. While the analysis Yuan and Hicks [16] were in 2D, a detail 3D analysis merit further studies to determine this behaviour. Results shows that the coupled temperature-pore pressure element can be used for the electro-osmotic consolidation of the soil.

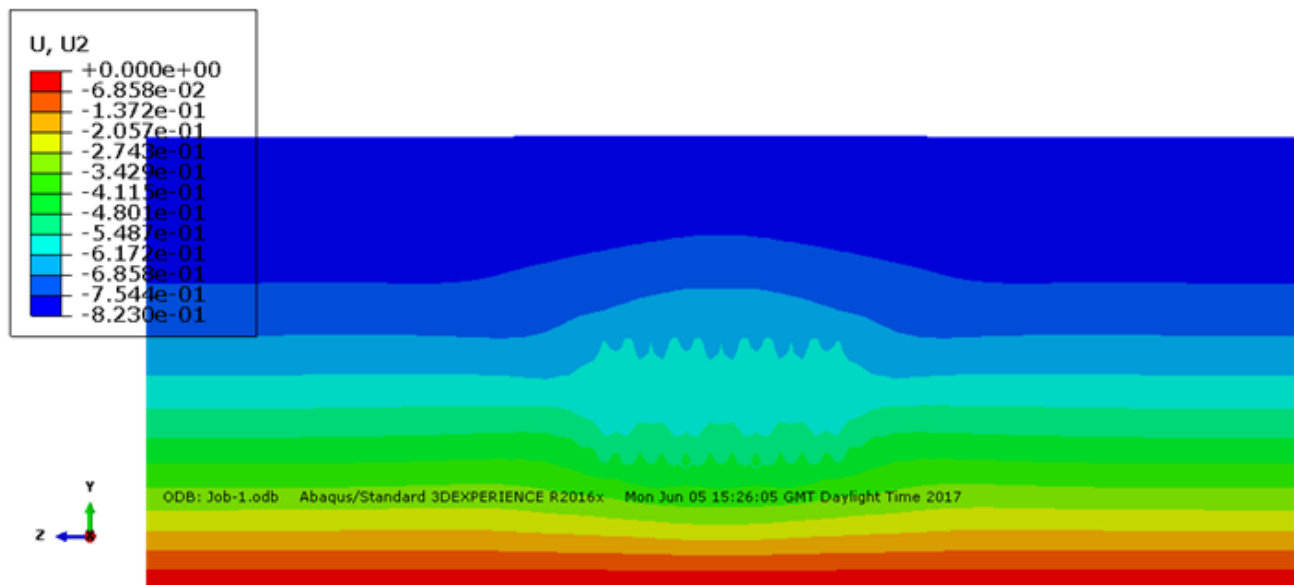


Fig. 13 Phase-2: Soil Settlement

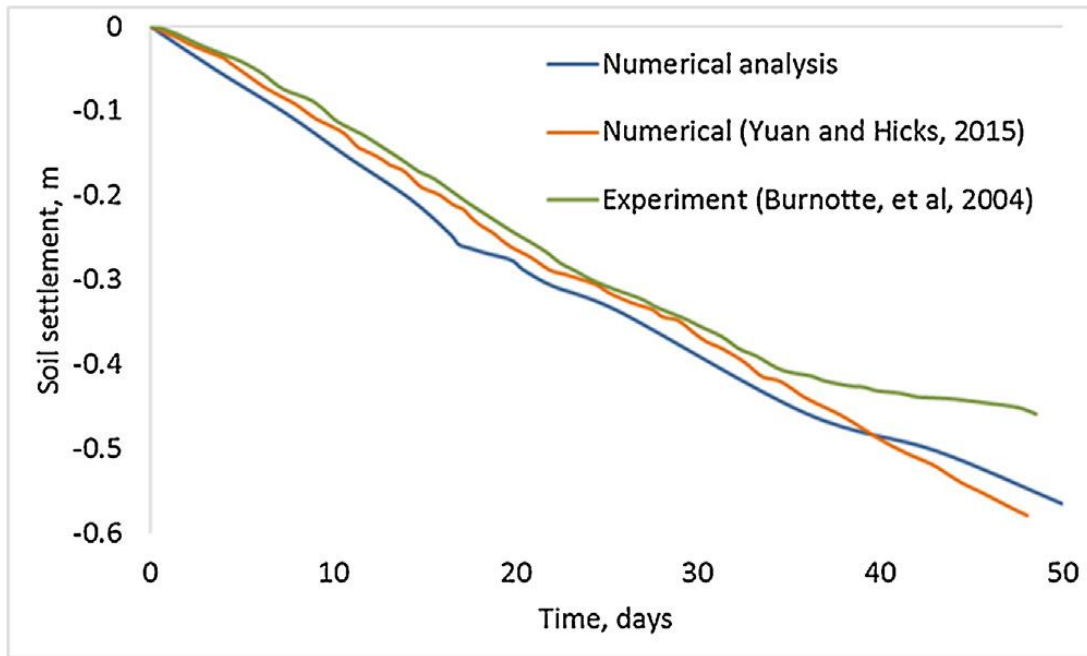


Fig. 14 Phase-2: ABAQUS validation of coupled temperature-pore pressure element for electro-osmotic analyses

3.3 PHASE-3: EK Pipe-Soil Interaction Model

Flow behaviour of test model are presented. The nodal temperature (NT11) shown in Fig. 15, mimic the voltage (V). Electrical field distribution from anodes to cathodes is shown in Fig. 15 and the flow behaviour below the pipe surface is also described in Fig. 16. The distance of 0.19m between the anodes and cathodes, along the pipe surface forms the effective voltage gradient as described in Fig. 16. Assuming from the distance of 0.19m between the anode and cathode as described in Fig. 16 a potential gradient of approximately 13V/m for the 2.5V and 132V/m for the 25V is developed. The greater the voltage, the higher the gradient for same distance in consideration.

Areas embedded with anodes have the same potential of 10V and consequently decreases to below 2V around the cathodes area as the excess pore pressure is drained into the water. The flow shows a steady decrease in voltage up to point 0.1m and then maintained a steady state of 1.7V. The behaviour at this point is attributed to flow from the soil region into the seawater region.

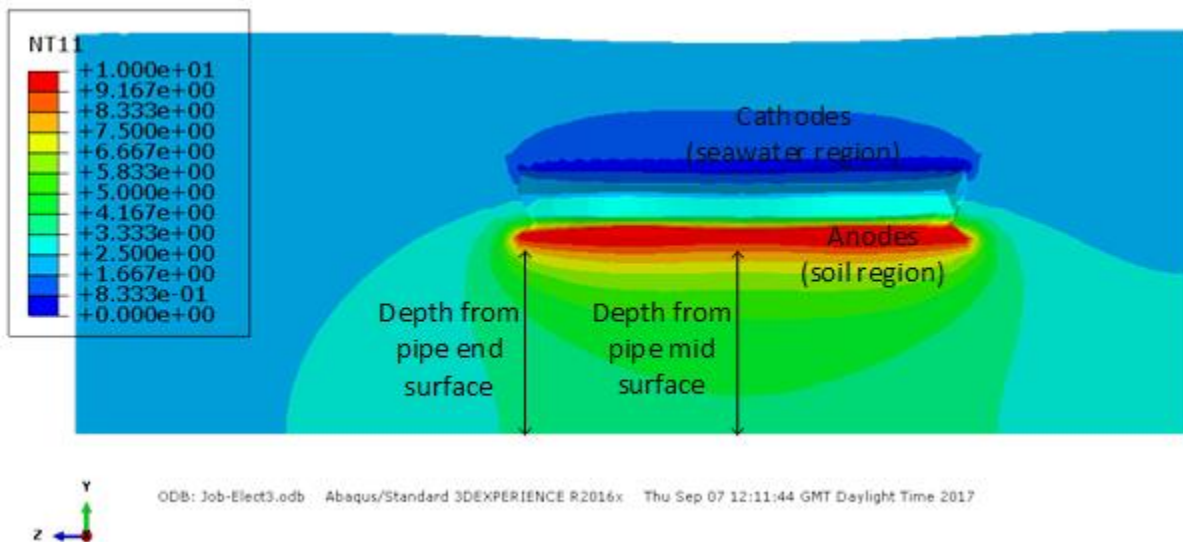


Fig. 15 Contour plot showing section view of electrical field distribution during the electro-osmotic flow process

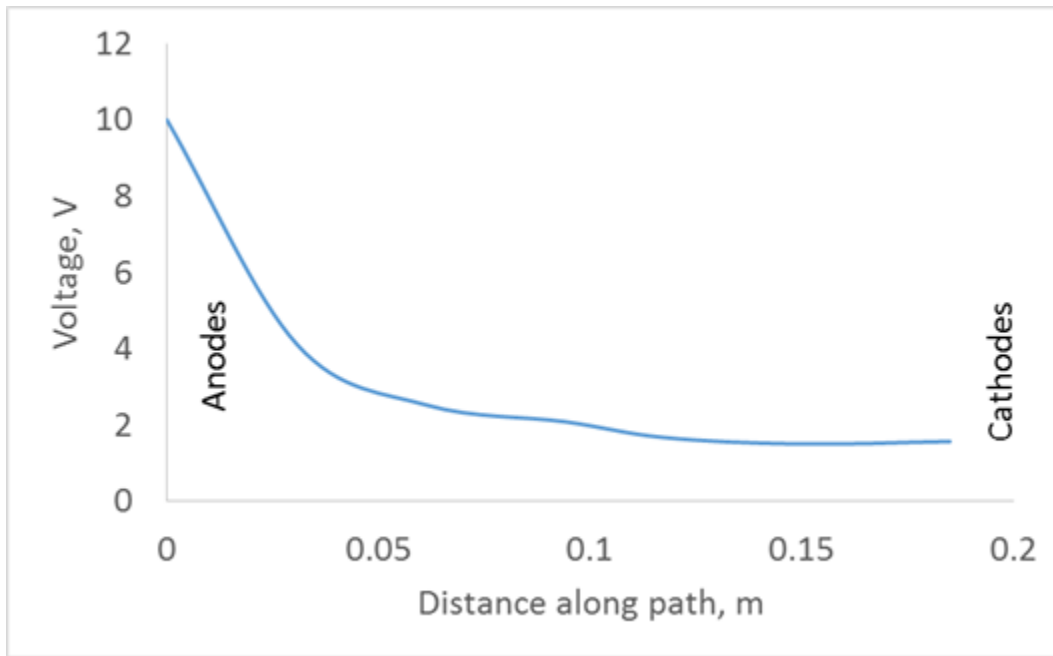


Fig. 16 ABAQUS electrical field distribution during the electro-osmotic flow process

3.3.1 EK Area of Influence

The electrical field distribution on the soil determines the area of influence. Area of influenced due to EK soil treatment spread to a depth below the pipe as the potential at the soil surface is assumed to be less than the anodes. Fig. 17 shows that the EK influenced in the soil extended to a depth of about 0.35m. The greater influence are experienced from the mid surface of pipe than from end surface. The flow on each of the surfaces shows a continuous decrease in flow concentration with depth. The midpoint of the pipe shows decrease in the flow concentration to less than 4.1V while the end point decreases to 3.5V. A voltage difference up to 0.6V is experienced within these areas. The voltage is more concentrated within the centre surface of the pipe than at the end point of the pipe surface. This can be attributed to the enclosure, as the end surface of the pipe have least resistance to flow than at the midpoint.

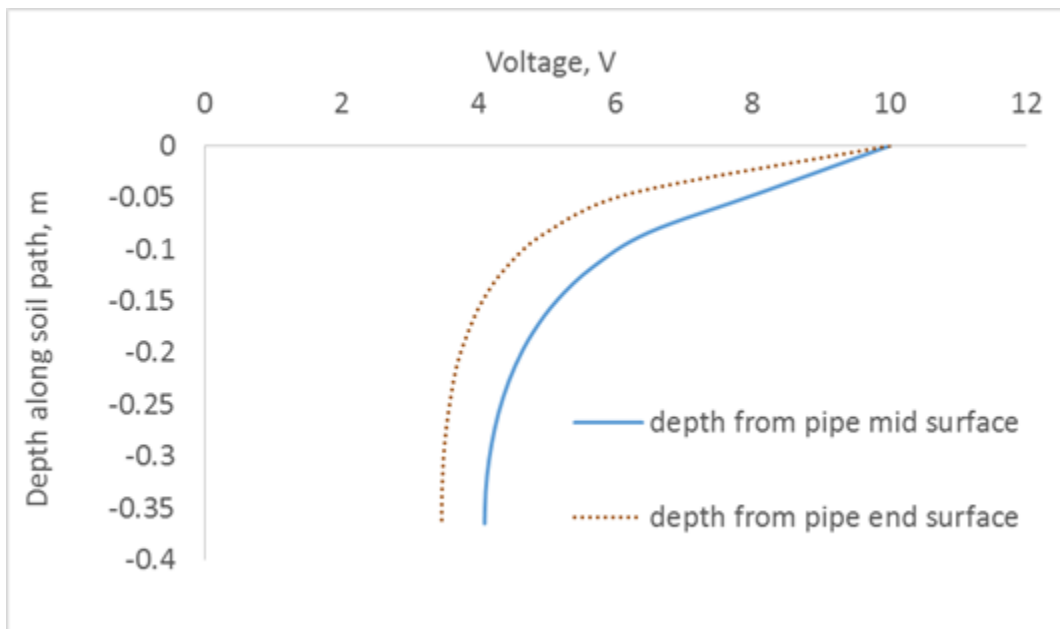


Fig. 17 Area influence by electrical field flow from pipe invert surface

3.3.2 Soil Pore Water Pressure

Voltage gradient $i_e = \frac{\partial \phi}{\partial x}$ in Table 1 created due to spacing of 0.19m between the anodes and cathodes as show in Fig. 16, has been the driving force for the voltage and pore water u_e , dissipated from the soil. The positive pore water pressure is experienced within the soil and shows gradual decrease as it move towards the cathodes as shown in Fig. 18.

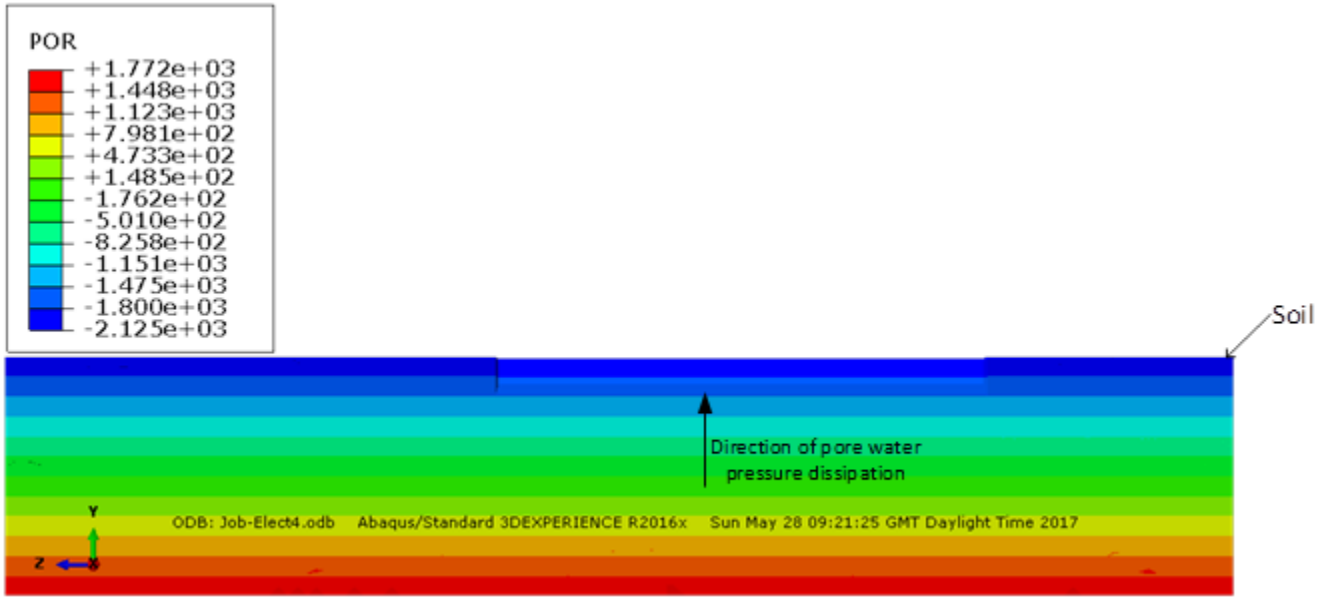


Fig. 18 Contour plot showing section view of pore pressure distribution within the soil

The dissipation of positive pore water pressure from the soil void led to decrease in the soil void ratio from 1.5 to 0.79 as shown in Fig. 19. The positive pore water pressure decreases and tend to be negative mainly around the anodes region to a depth of 0.24m as shown Fig. 20.

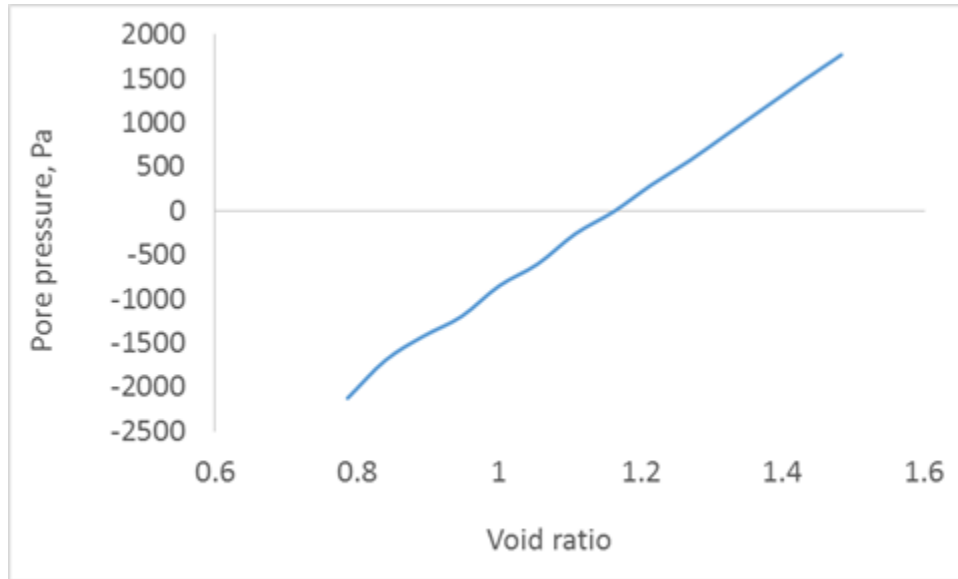


Fig. 19 Effect of pore water pressure dissipation on soil void ratio

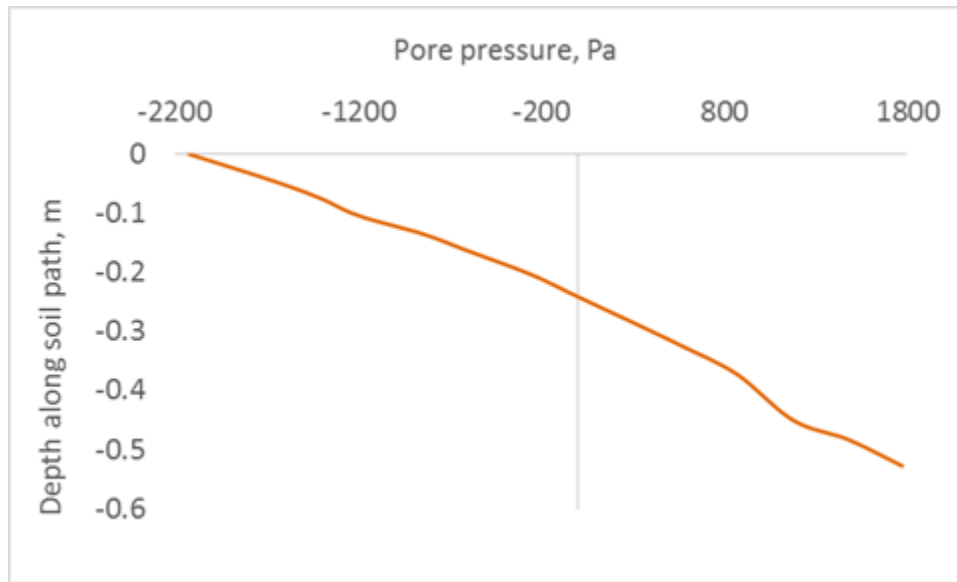


Fig. 20 Pore water pressure distribution within the soil

3.3.3 Soil Effective Stress Distribution

The build-up of negative pore water pressure resulted from the expulsion of pore water from the soil void. This process led to the decrease in the void volume. The resultant decrease in soil volume accounted for the increase in soil effective stress as shown in Fig. 21. The soil effective stress distribution in Fig. 22 indicated steady increase within the pipe invert perimeter from a depth of 0.1m. The vertical effective stress is affected by its closeness to the treatment zone near the anode and the settlement of the soil due to its own weight. This signifies an improvement in the soil strength near the treatment zone. As the depth increase, the effective stress is also noticed to increase, this behaviour can be attributed to the soil properties which indicates higher strength gradient with depth than the upper layer.

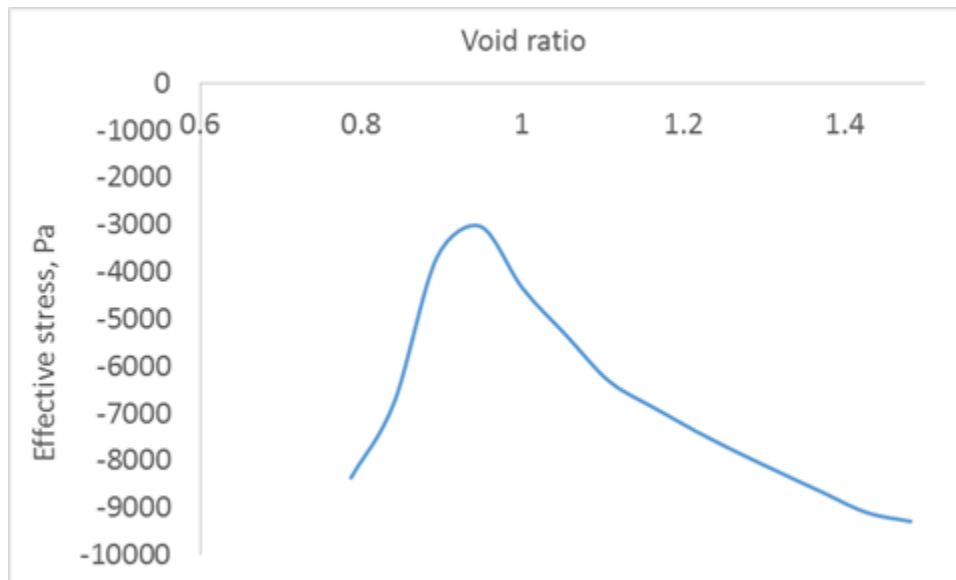


Fig. 21 Effect of vertical effective stress on soil void ratio

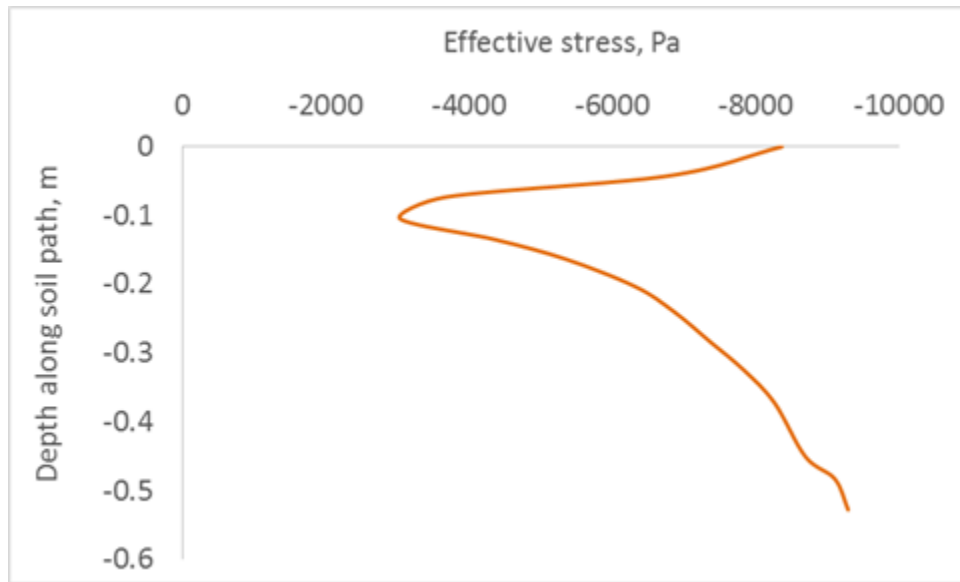


Fig. 22 EK effect on soil effective stress distribution within the soil

3.3.4 Steady State Analyses: Soil Settlement

Soil settlement occurs due to removal of pore water from the soil. For the non-EK process with no applied voltage, a maximum soil settlement of 0.002945m is observed as shown in Fig. 23. For the EK process, the soil experiences a maximum vertical settlement of 0.01872m after subjecting it to a steady state consolidation process as shown in Fig. 24. The settlement is much more experienced beside the pipe surface. The resultant effects of the electro-osmosis on pipe-soil interactions are discussed further in the dynamic analyses section.

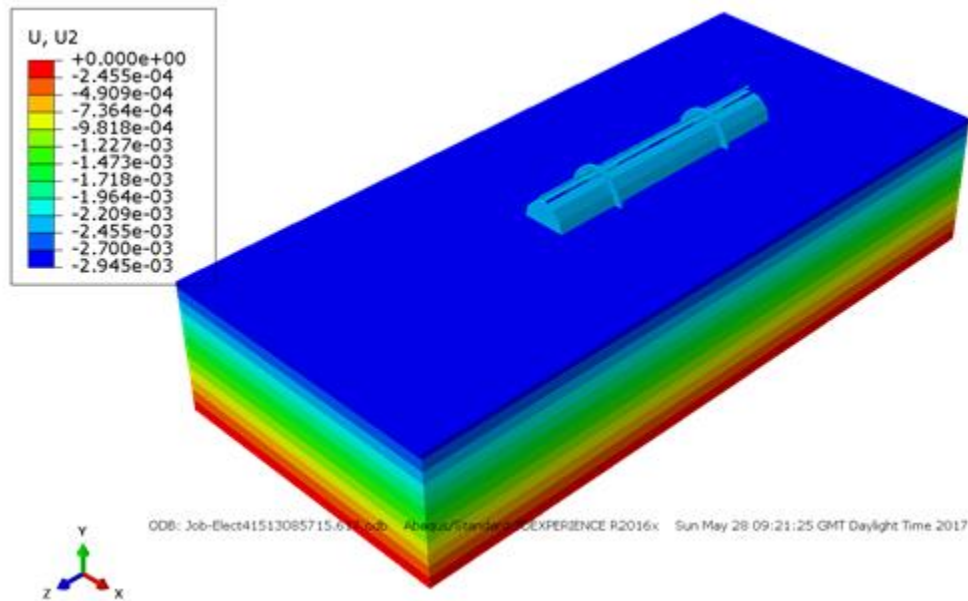


Fig. 23 Section view of vertical soil settlement distribution within the soil due to non-EK

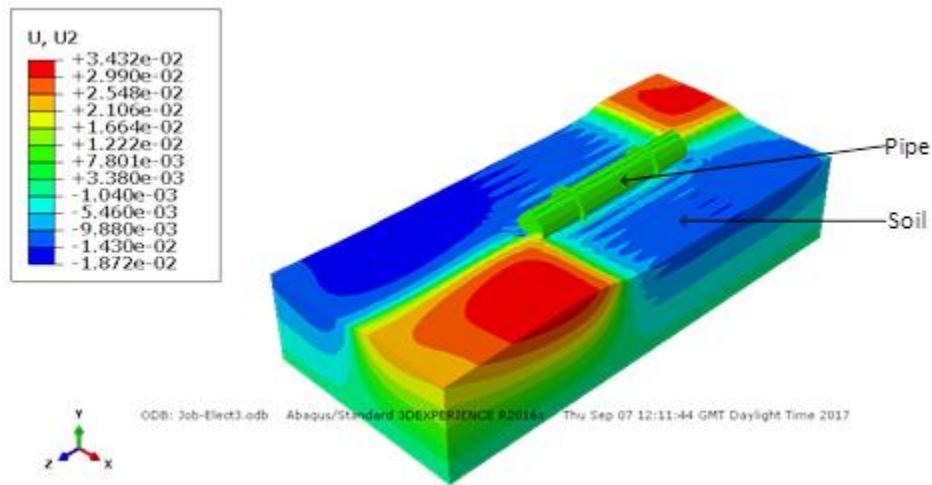


Fig. 24 Section view of vertical soil settlement distribution within the soil due to EK

The higher voltage concentration at the anodes allows for the flow to move towards the cathodes being the surface with lower concentration. Fig. 16 shows the flow behaviour to be more effective at a distance of 0.19m from anodes to cathodes areas. The effect of treatment does not span through all the soil regions, small area is being affected when compared with the whole model. However, as given in [10], the continues iron diffusion after treatment allows for soil consolidation to continue, which is considered to be a permeant process. This may take care of the potential flow reversal, which has not been captured in this study and may be a factor to be considered in further studies. The reduction in the soil void is due to the dissipation of pore water pressure from the soil which led to the increase in effective stress experienced in the soil as given in Fig. 22. This phenomenon has been given in Eqn. 7.

3.3.5 Steady State analyses: Effect of Voltage Variation

Steady state analyses with voltage variation were also indicated in Fig. 25. Applied voltage of 2.5-25V were tested, result indicates a gradual settlement of the soil with increase in voltage. The least settlement can be notice for the 2.5V with the highest settlement for the 25V.

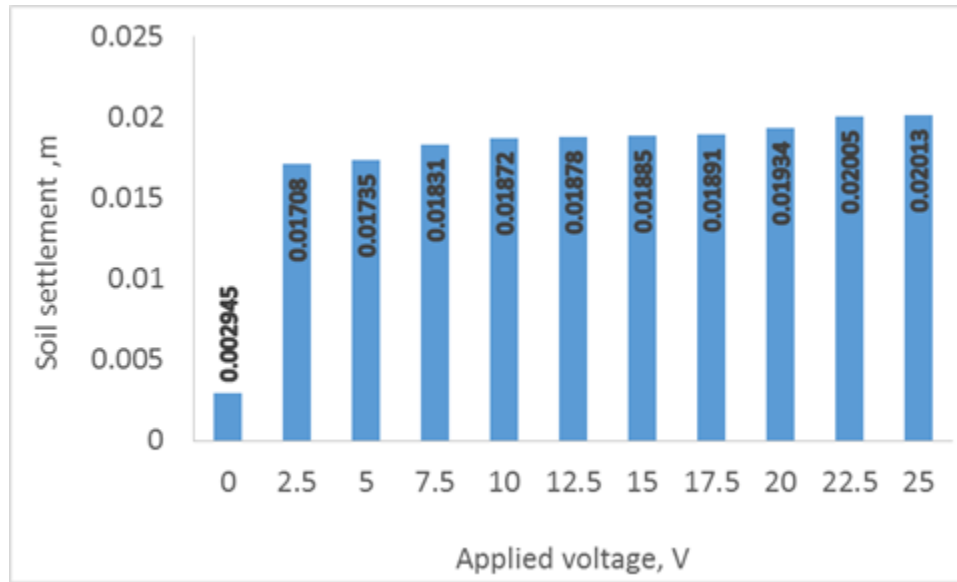


Fig. 25 Steady State analyses showing effect on soil settlement due to voltage variation

3.3.6 Transient Analyses: Effect of Treatment Time

The results from Fig. 26 indicates the effect of soil settlement due to treatment time. A voltage of 10V is applied for all the treatment time. The soil indicates a progressive settlement of 0.00528m for 6 hour, 0.00972m for 12 hour, and 0.01328m for 24 hours. From Fig. 26, a 3.5% increase in settlement between 6-hours and 12-hours, and 18% between 6-hours and 24-hours is observed. The significant

increase with time underscore the importance of treatment time to soil consolidation. The greater time taking, allows iron diffusion to be more effective aimed at hardening of the soil with greater impact on the soil strength.

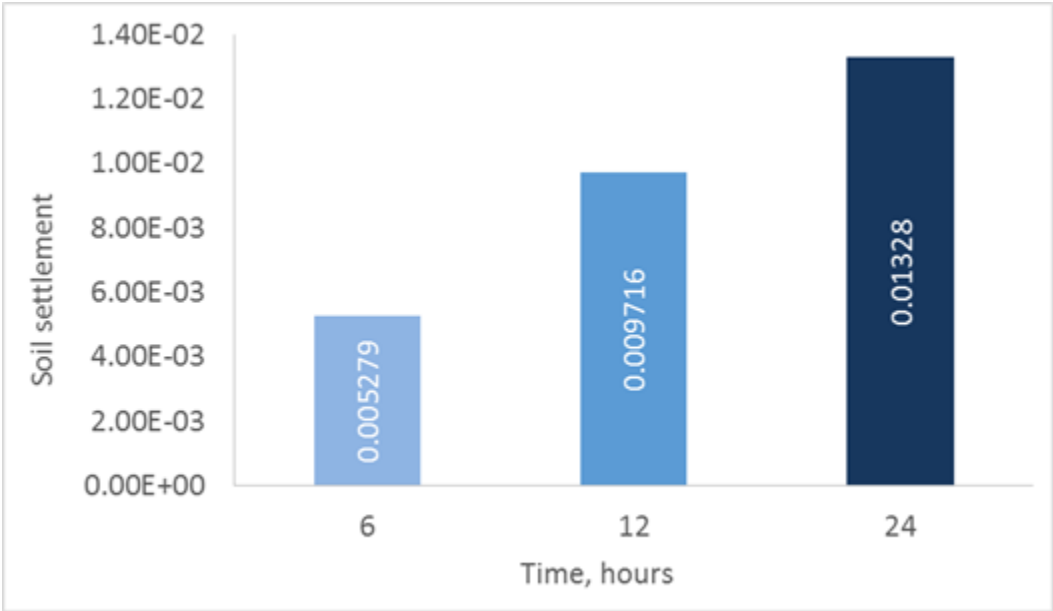


Fig. 26 Effect of treatment time on soil settlement

3.3.7 Transient Analyses: Effect of Voltage Variation

The effect of voltage variation on soil settlement are presented. The results as shown in Fig. 27 indicates soil settlement is affected with variation in the applied voltage. The soil settlement shows gradual increase from 2.5V to 25V. This is attributed to small area being affected in the soil when compared with the whole soil dimensions. This behaviour indicates the feasibility of using lower voltage to give approximately same effect as with higher voltage with consideration to treatment time as previously shown in Fig. 26. Although the soil settlement experience is of little fraction when compares with the increasing voltages, this is enough to cause significant changes in the soil strength as discussed further in the dynamic analyses section.

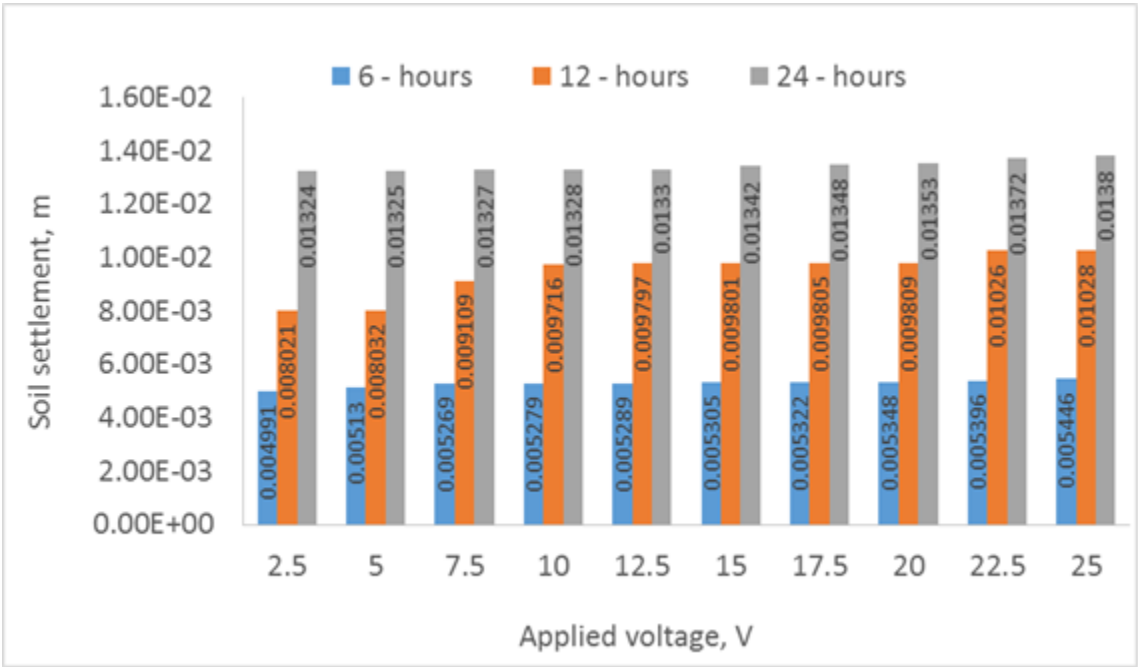


Fig. 27 Transient analysis showing effect on soil settlement due to voltage variation

4 DYNAMIC PIPE-SOIL INTERACTION ASSESSMENT

Investigation of the dynamic analyses of the pipe-soil interaction are based on comparisons between non-EK and EK treated soil, which are presented in this section. The test model indicates results due to soil settlement with variation in voltage, time, and forces developed due to vertical penetration, axial and lateral pulling of the pipeline. Results of steady state analyses in vertical, axial and lateral directions were also presented.

4.1 Steady State Analyses: Effect on Pipe Vertical Penetration

Pipeline vertical penetration behaviour is shown in Fig. 28. Being a WIP pipe, the formation of heave around the pipe surface is minimal. Greater penetration force and behaviour may be experience for a PIP than WIP pipe due to formation of heave within the soil perimeter. Heave formation increases the pipe contact area with a resultant increase in resistance to displacement. However, as initially stated in previous section, the WIP pipe is adopted to allow for anodes-soil contact. The comparison of non-EK and EK process under same condition as shown in Fig. 31 defines the effect electro-osmotic consolidation have on pipe displacement. Penetration velocity of the pipeline as described in Fig. 29 indicates slight fluctuations with depth.

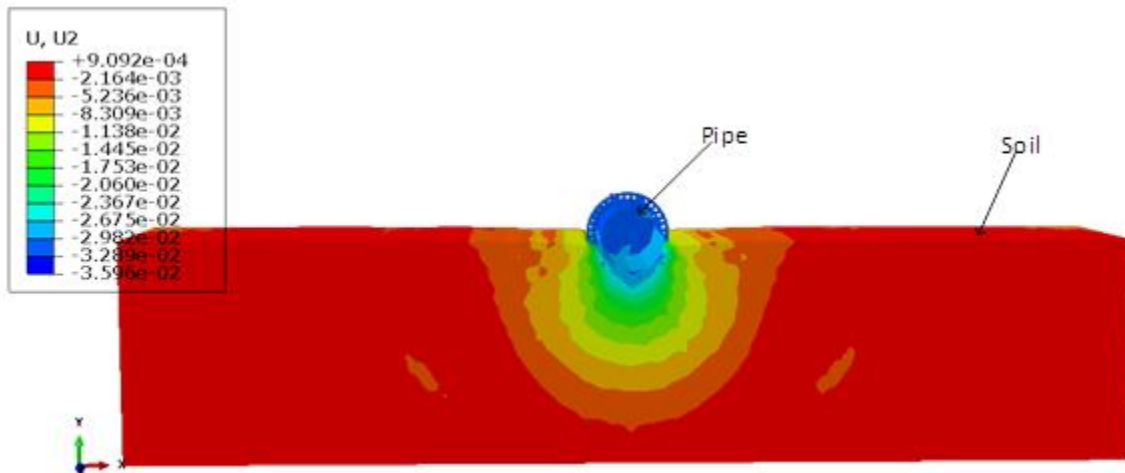


Fig. 28 Section view showing contour plot of pipe vertical penetration

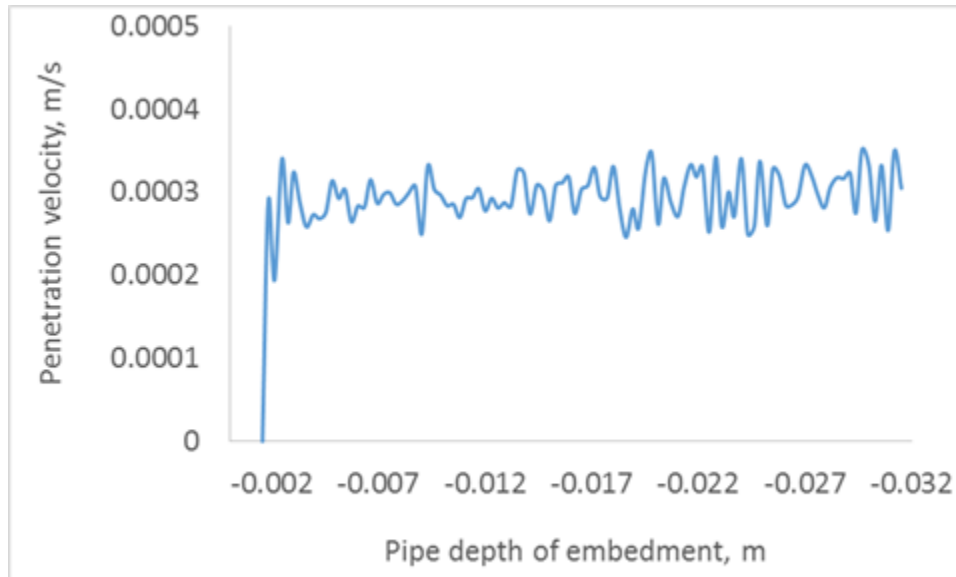


Fig. 29 Pipe penetration velocity with depth

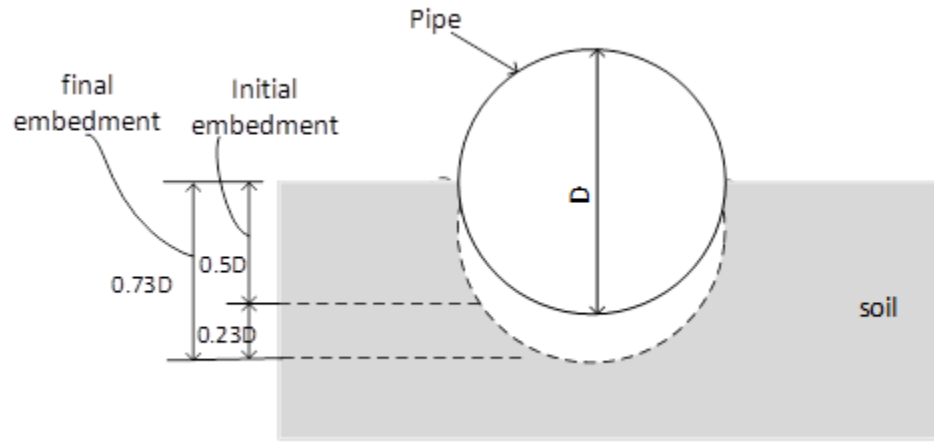


Fig. 30 Description of pipe embedment due to vertical penetration

Fig. 30 shows the initial and final position of the pipe embedment at $0.5D$ and $0.73D$ respectively. The reaction of the pipeline due to vertical penetration into the soil is shown in Fig. 31. The penetration behaviour shows gradual increase in resistance with embedment of pipe. For the non-EK process, the penetration force increases to $79N$ before breaking at a depth of $0.083m$ ($z/D = 0.64$) while the EK process shows increase of $160N$ before breaking at $0.081m$ ($z/D = 0.62$). The pipe vertical penetration indicates approximately over 103% increase in the penetration force due to EK treatment of soil.

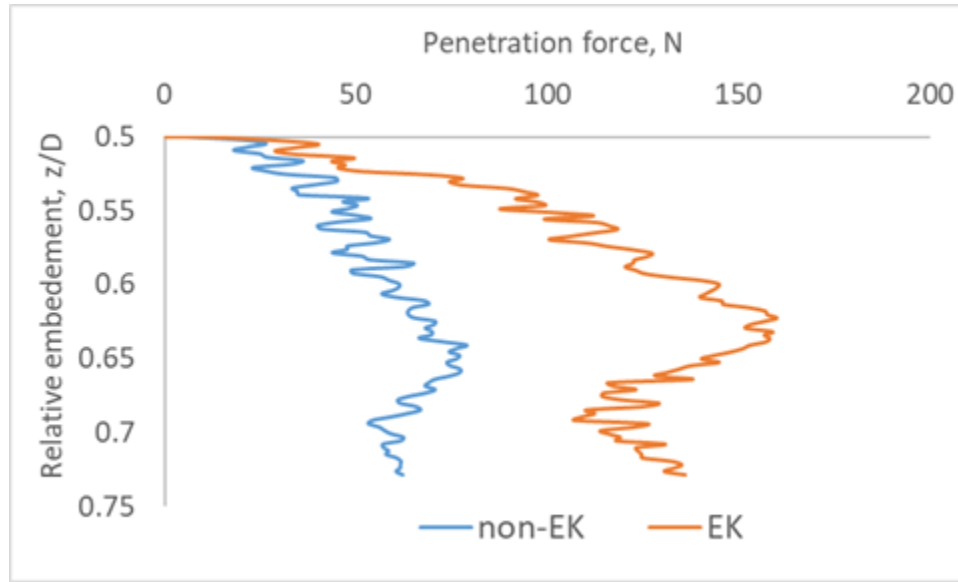


Fig. 31 Forces developed due to pipe vertical penetration with depth

4.2 Steady State Analyses: Effect on Pipe Axial Displacement

The pipeline shows axial displacement with uniform velocity. At the initial embedded depth of $0.065m$ ($0.5D$), the pipe experiences gradual penetration to the final embedment of $0.1m$ ($0.77D$) as described in Fig. 32 and Fig. 33. The embedded depth increase as the pipe moves away from the EK treated zone. The force-displacement behaviour is described further in Fig. 34.

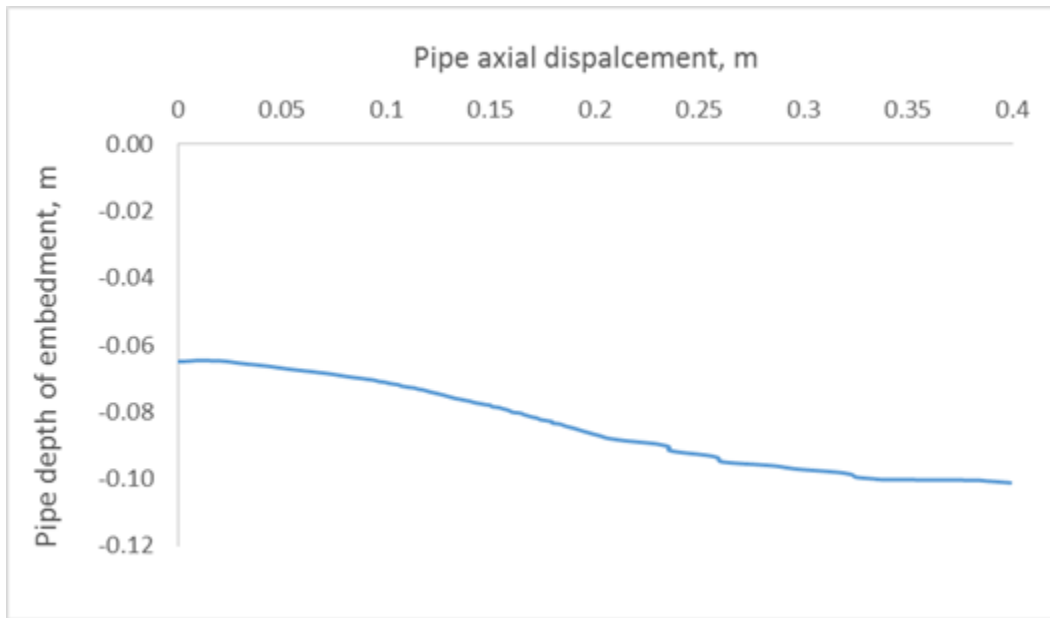


Fig. 32 Embedment of pipe due to axial displacement

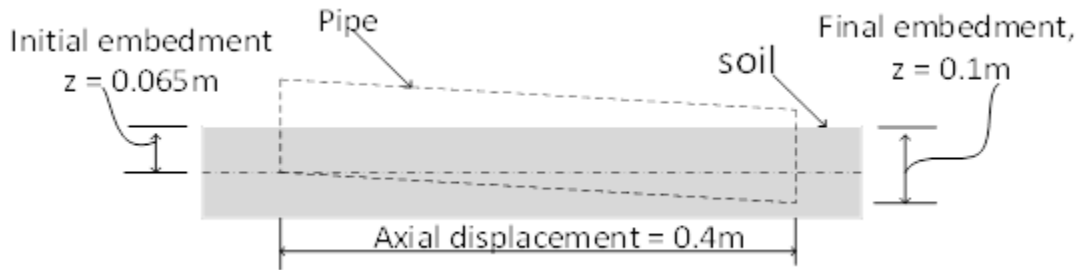


Fig. 33 Description of pipe position due to axial displacement

Axial test of the pipe-soil interaction were executed on non-EK and EK treated soil under same conditions. Results obtained were compared with experiment performed by Eton [4]. From Fig. 34, the non-EK treated soil experiences high initial stiffness tangent which gradually reduces towards the breakout (peak) force of 93N at distance of 19mm, greater than 63N obtained by Eton [4]. At the peak resistance, the breakout force rapidly decayed to a residual force. However, the EK treated soil, experiences a peak force of 207N at distance of 37mm, more than 182 obtained by Eton [4]. The dominant resistance is the residual force, steadily experienced throughout the duration of pipe displacement. Hence, this determines the behaviour of pipe displacement due to the effective force.

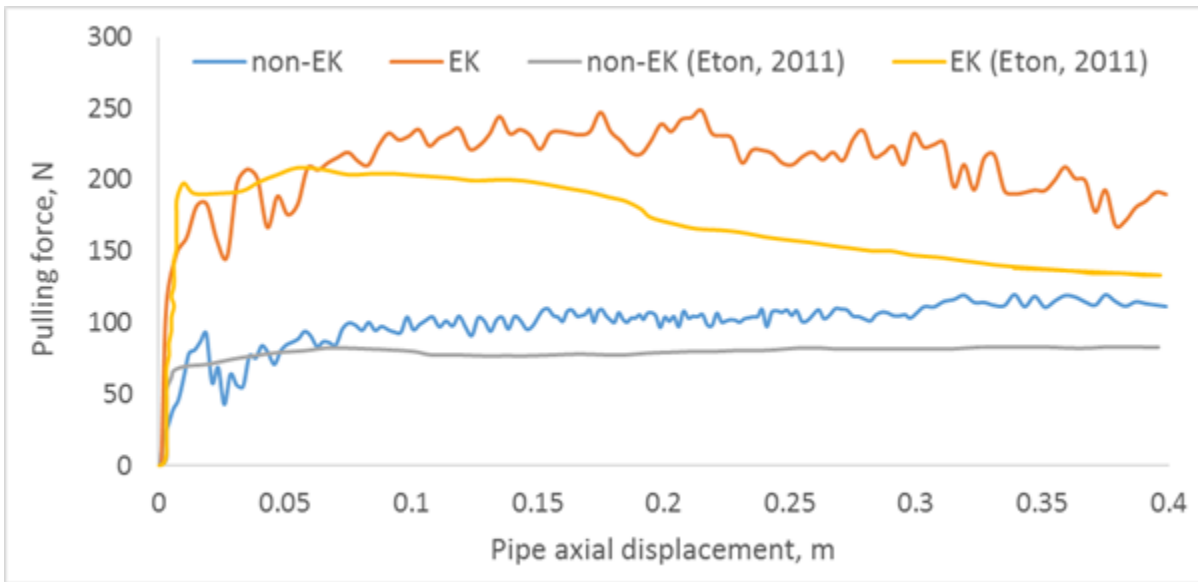


Fig. 34 EK effect on axial pipe displacement

A comparison between EK and non-EK treated soil for the axial displacement of pipe; a 123% increase in the breakout force is achieved as shown in Fig. 35.

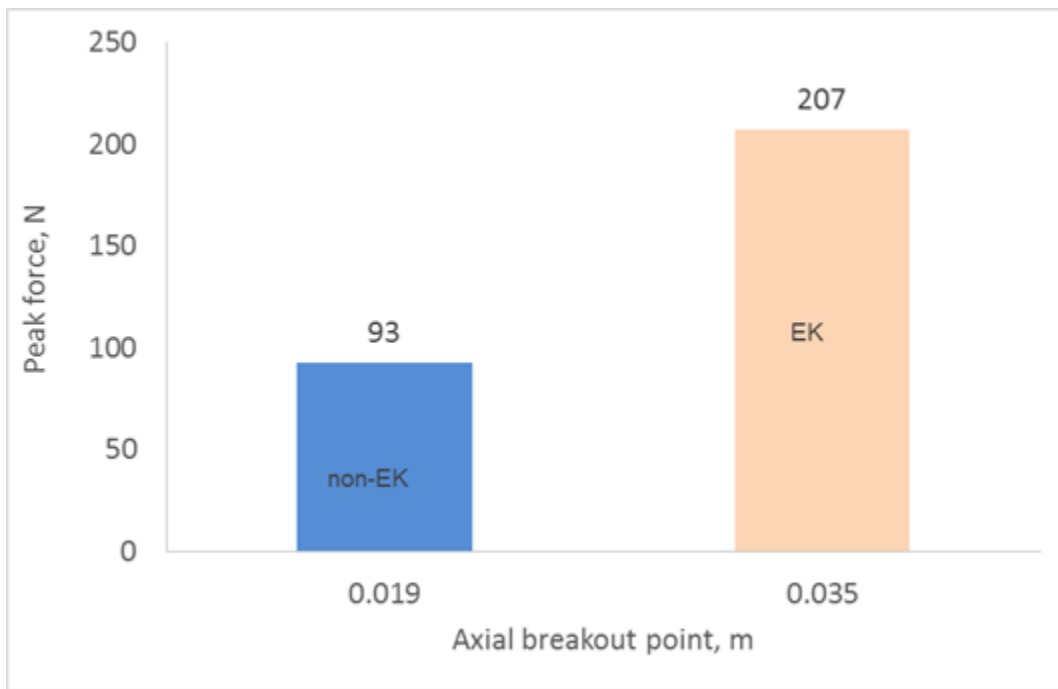


Fig. 35 Non-EK vs EK axial breakout force

4.3 Steady State Analyses: Effect on Pipe Lateral Displacement

The pipe displaces laterally with uniform velocity. The lateral displacement account for the pipe final embedment at 0.146m (1.12D) from its initial WIP position as shown in Fig. 36 and Fig. 37. The pipe embedment indicates increase as the lateral displacement moves away from the treatment zone. The resultant effect on resistance developed against pipe displacement is shown in Fig. 38.

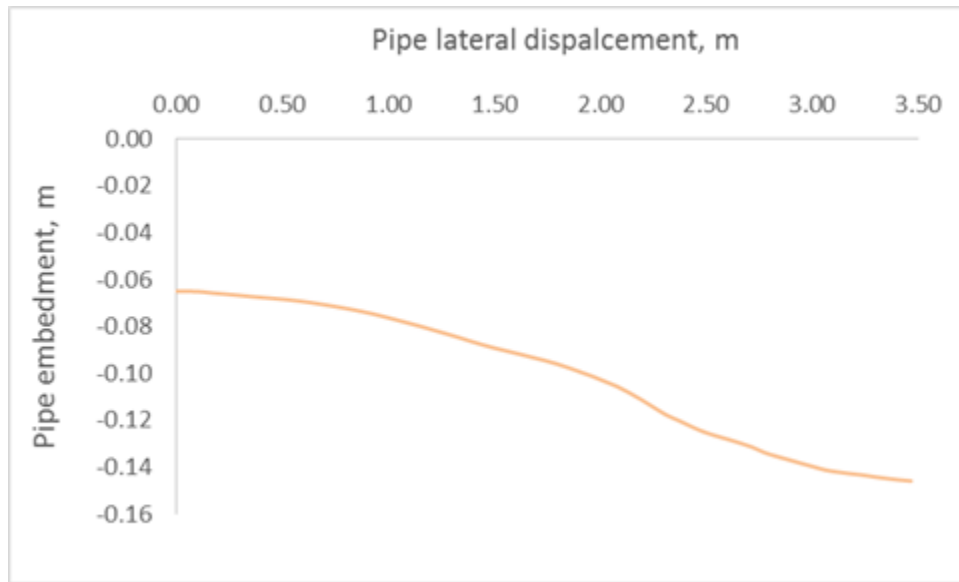


Fig. 36 Embedment of pipe due to lateral displacement

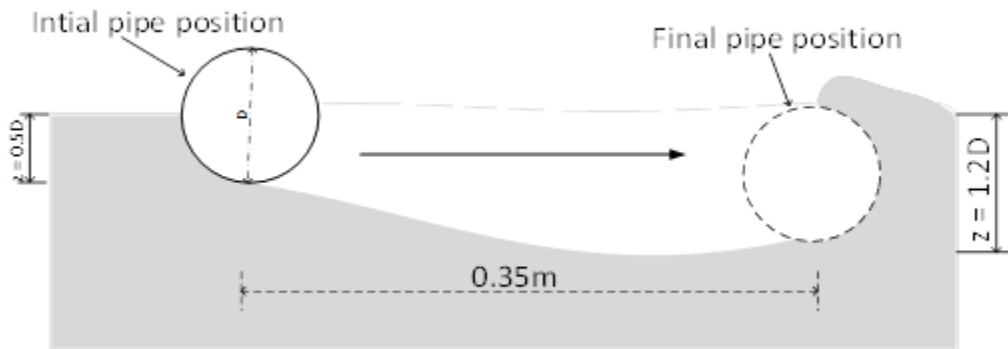


Fig. 37 Description of pipe position due to lateral displacement

The lateral displacement of the pipe on both non-EK and EK treated soil and the corresponding resistance is shown in Fig. 38. Results obtained were compared with experiment performed by Eton [4]. The behaviour shows similar trend with the axial pipe displacement. A comparison between the numerical and the experimental result shown in Fig. 38, the numerical model indicates higher peak force of 11% for the EK treated soil than the experiment.

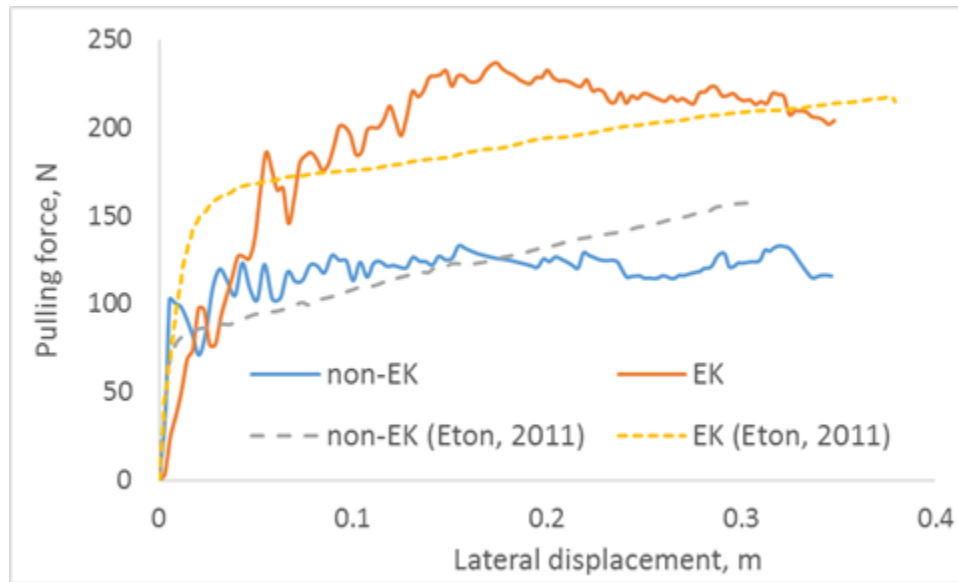


Fig. 38 EK Effect on lateral pipe displacement

Fig. 38 shows a breakout force of 103N occurs at a distance of 5mm for the non-EK treated soil greater than 81N obtained from the experiment and 186N for the EK treated soil at 55mm greater than 168N obtained from the experiment. A comparison between EK and non-EK, shows over 81% increase in the soil resistance as shown in Fig. 39.

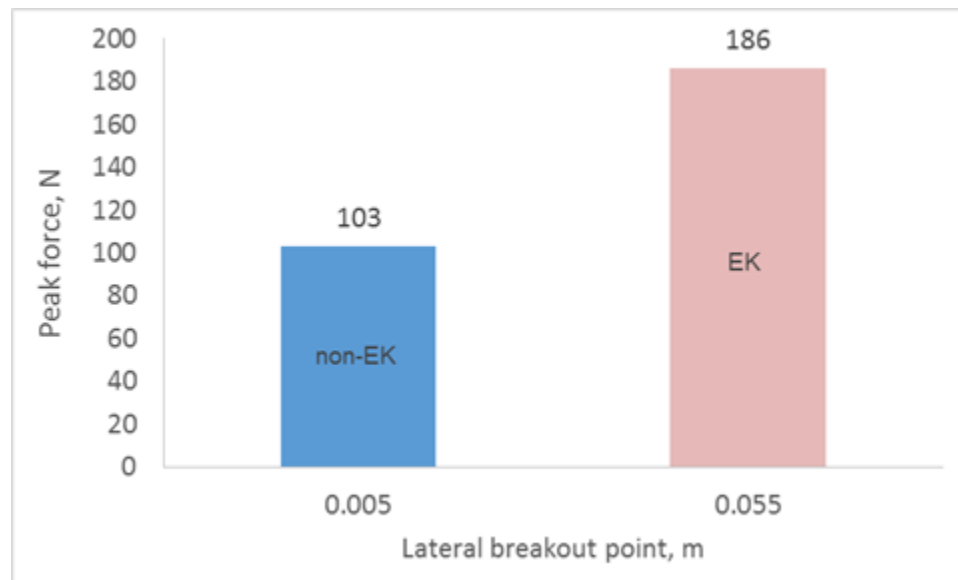


Fig. 39 Non-EK vs EK lateral breakout force

4.4 Transient Analyses: Effect of Treatment Time

The resultant effect on pipeline displacement in axial direction due to treatment time is shown in Fig. 40. The axial pulling force developed indicates the influence of treatment time on soil consolidation. The soil undergoes a treatment time of 6, 12, and 24 hours at a constant voltage of 10V. As the treatment time increases, the soil settlement also increases. Due to the soil settlement, axial pulling force required to pull the pipeline increases with the treatment time. This signifies improvement in the soil strength. The pulling force for each of the treatment time is characterised by a peak force and a residual force behaviour discussed in previous sections. As given in Fig. 40, the peak force being generated increases from 93N for non- EK treated soil to 143N, 146N, and 148N for 6 hour, 12 hours, and 24 hours for EK treated soil respectively.

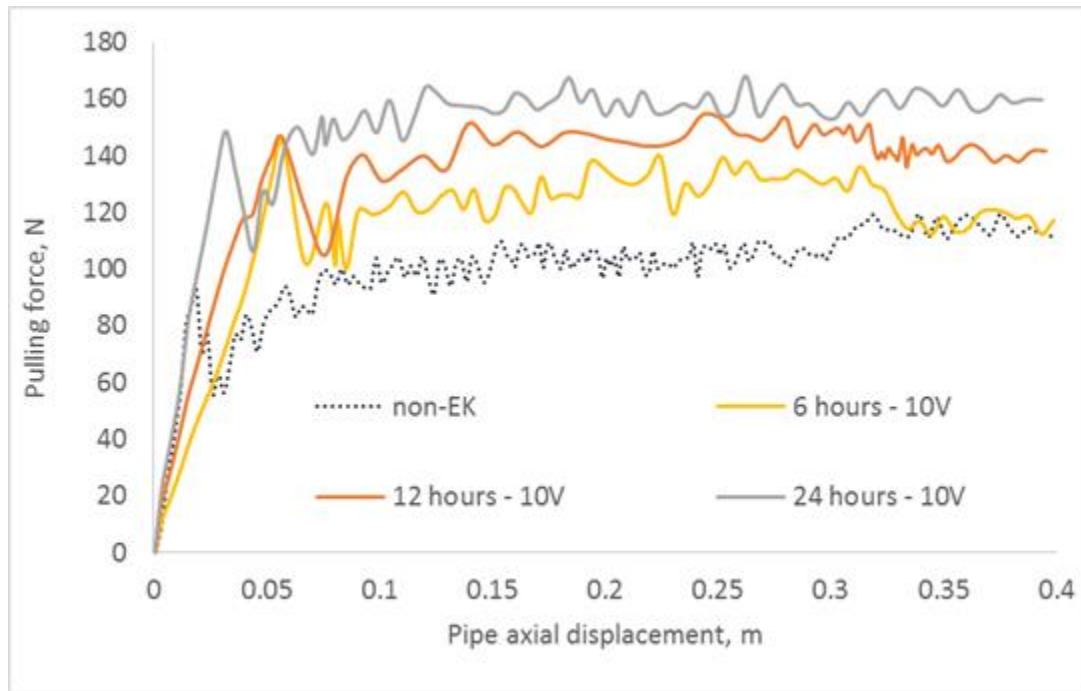


Fig. 40 Effect of EK on pipe axial displacement with time variation

Comparing the EK process for the varying time as shown in Fig. 41, the soil indicates an increase in the peak (breakout) force of 54%, 57%, and 59% for the 6-hours, 12-hours, and 24-hours treatment time respectively.

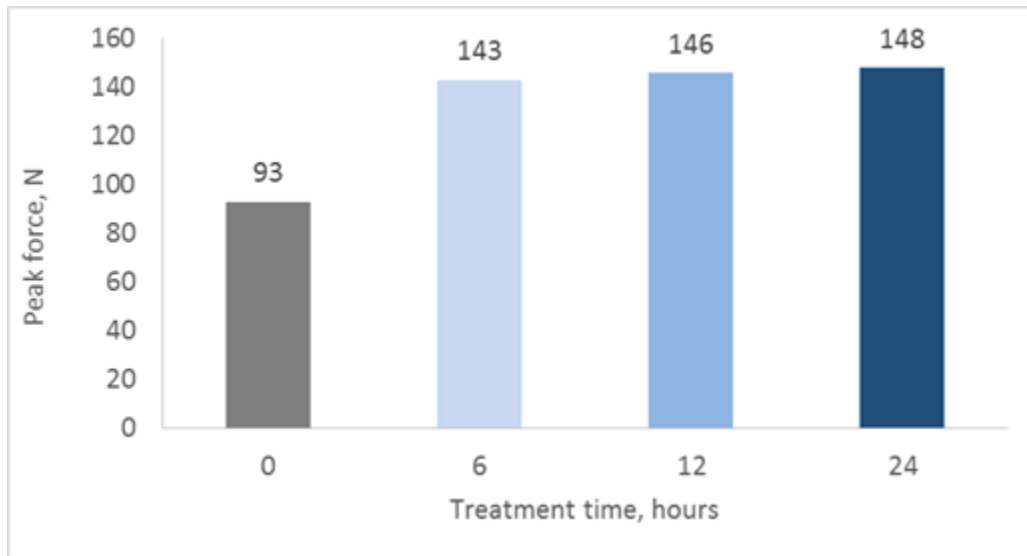


Fig. 41 Breakout forces developed with treatment time

4.5 Effect of Voltage Variation at Treatment Time of 6-Hours

Axial pulling force developed as shown in Fig. 42 indicates the significance of increasing voltage on soil settlement. The force required to pull the pipeline increases with increasing voltage due to improvement in soil strength because of the soil settlement described in Fig. 27. The soil undergoes a treatment time of 6 hours with increase in voltage from 0-12.5V. The pulling force is characterised with peak force and a residual force behaviour discussed in previous sections. As indicated in Fig. 42, the peak force for 0V (non-EK) is 93N however, as voltage is applied, the peak force increases to 136N, 143N and 144N for 7.5V, 10V and 12.5V respectively.

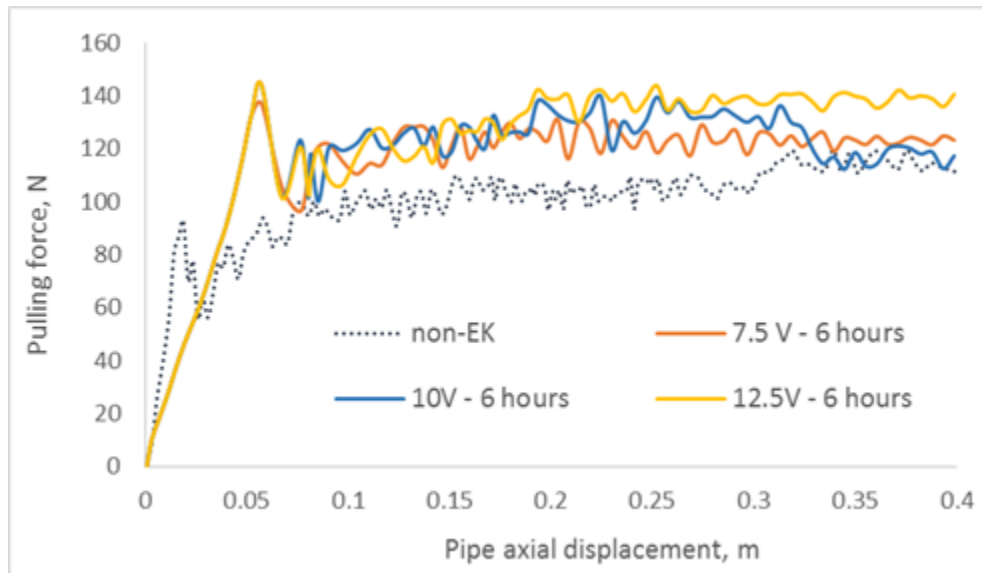


Fig. 42 Effect of soil settlement on pipe axial displacement with voltage variation at 6 hours

A comparisons between the EK and non-EK (zero voltage) as shown in Fig. 43; there is a 46%, 54%, and 55% increases in the peak force for the 7.5V, 10V, and 12.5V respectively.

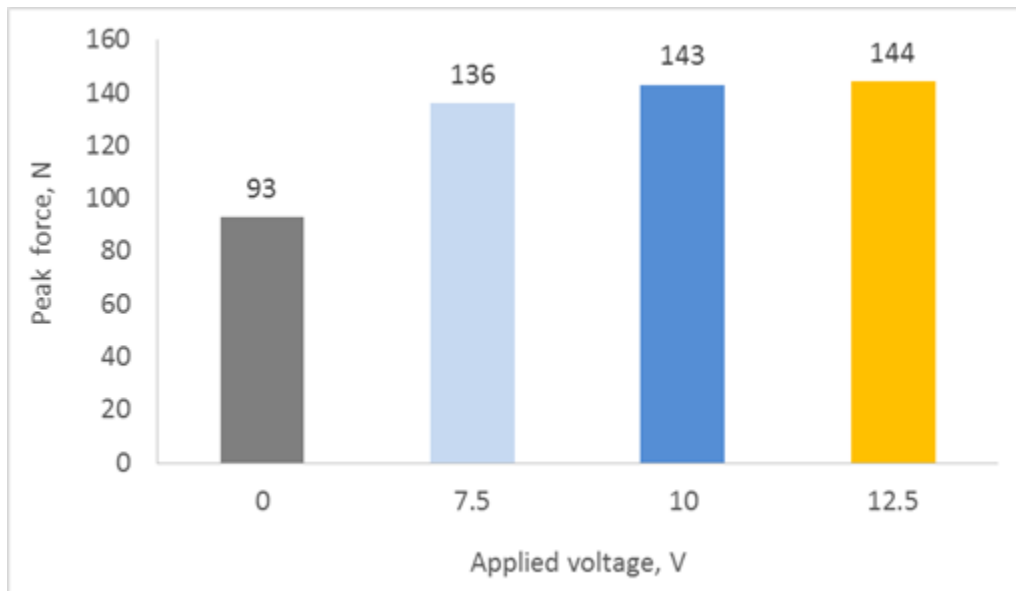


Fig. 43 Breakout forces with voltage variation at 6 hours treatment time

4.6 Effect of Varying Voltage at Treatment Time of 12-Hours

Further subjecting the soil to a treatment time of 12hours and varying the voltage from 2.5 to 12.5V, the soil indicates further improvement in the peak and residual force as shown in Fig. 44. Similar behaviours as previously described were observed. Fig. 45 indicate a peak force of 96N at 0V, as voltage is applied the peak force increases to 143N, 143N and 145N, 146N and 146.6N for 2.5V, 5V, 7.5V, 10V and 12.2V respectively.

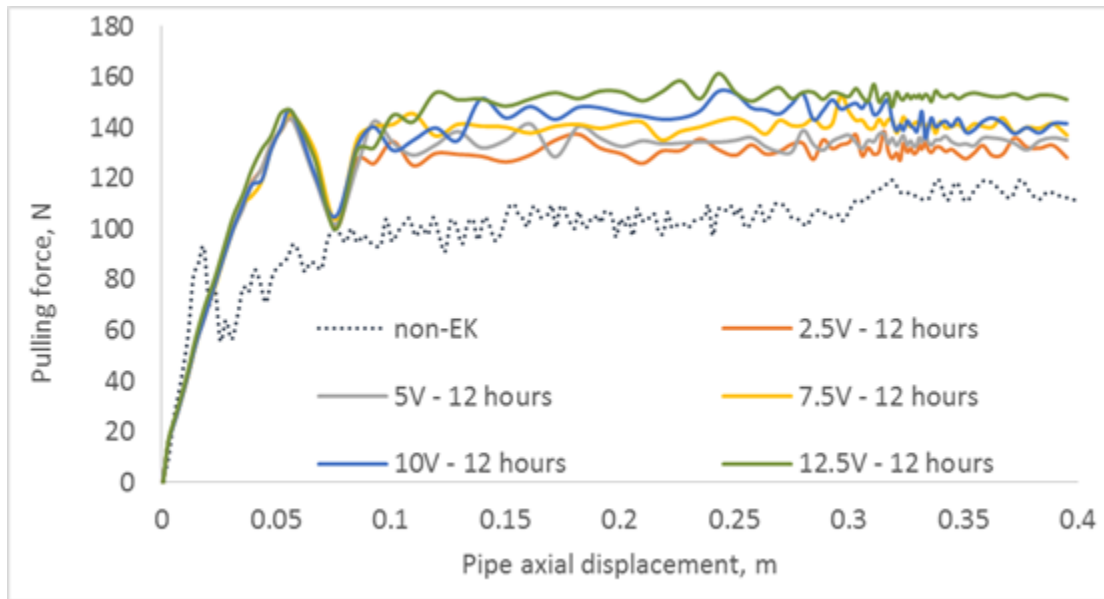


Fig. 44 Effect of soil settlement on pipe axial displacement with voltage variation at 12 hours

A comparison with the non-EK treated soil as shown in Fig. 45 indicates 54% increase in the axial pulling force for the 2.5 and 5V. Subsequent increase in voltage shows little increase with significant impact on the residual forces.

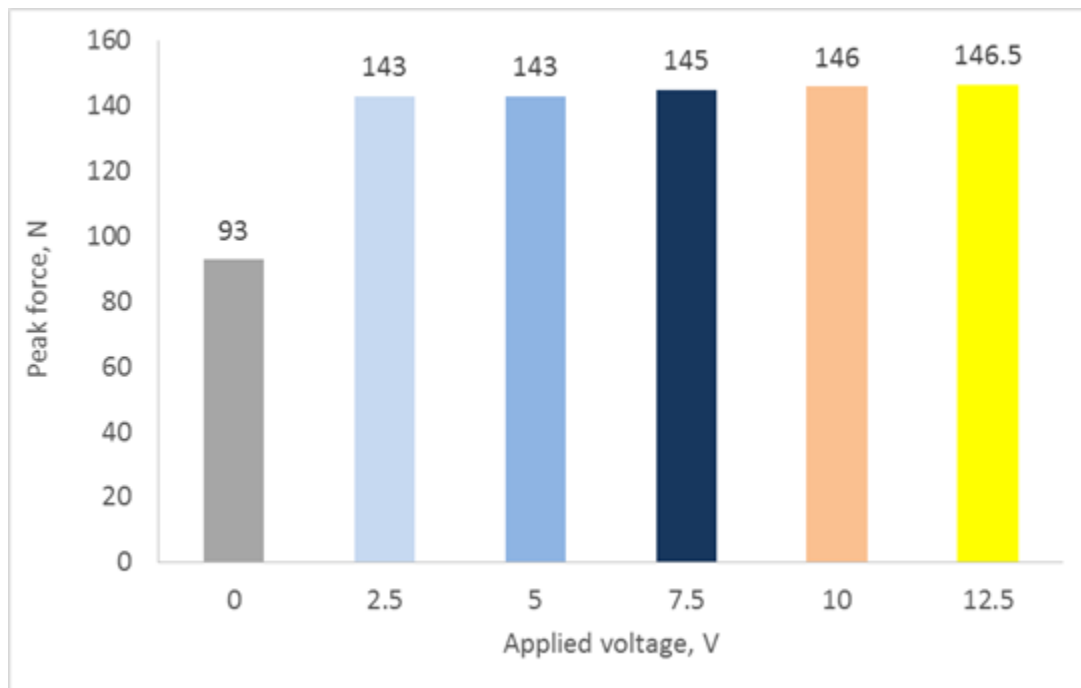


Fig. 45 Breakout forces with voltage variation at 12 hours treatment time

4.7 Possible Field Application

A possible mitigation against pipeline displacement is to increase soil resistance [1,3,55,56]. The EK effect has the potential at significantly improving soil strength to serve as a possible mitigating measure. As this is a new approach, it can be incorporated into a new offshore pipeline design. Other areas of possible application is the underwater cables. Assessment of the soil properties and the pipeline embedment during installation and in operating condition should be conducted. The assessment will help to determine the electrodes configuration and power requirement for each individual case. Assessment of electrochemical reactions with consideration to insulation of pipeline and inline structures from interfering with the EK reaction should be a priority.

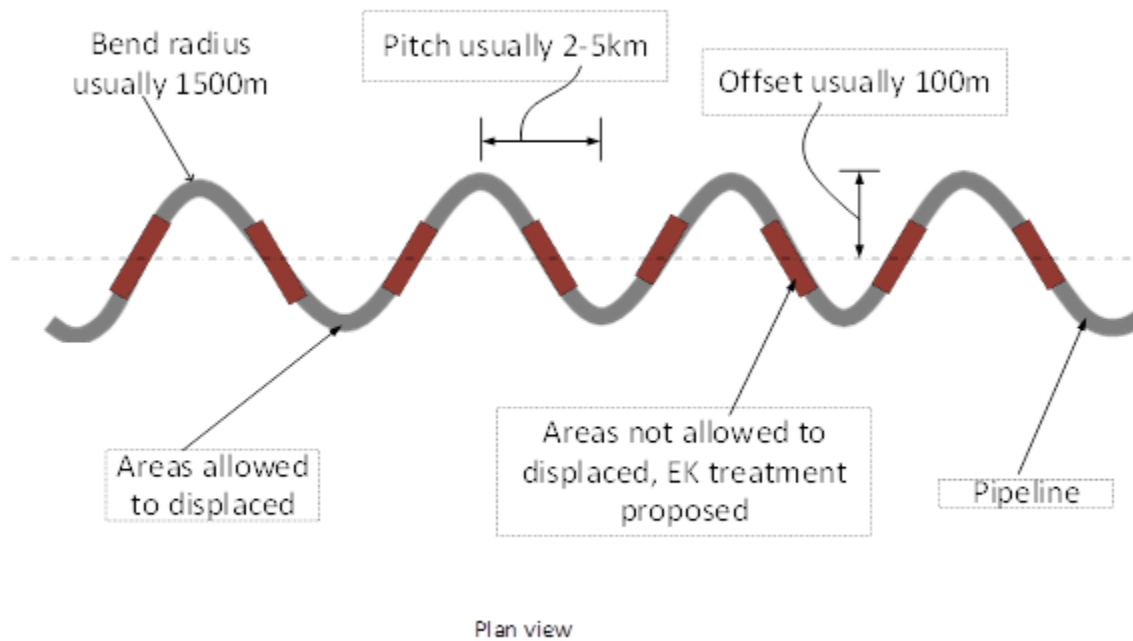


Fig. 46 Snake Lay of pipeline showing possible areas for EK treatment

As the EK process proves to be effective, it is recommended that the EK design may have electrodes attached to the pipeline or pre-installed at certain areas prior to pipeline installation depending on the field conditions and cost of operation. The Fig. 46 shows a snake lay of pipeline [57], this method helps to reduce axial displacement but with limitation in deep water due to uncertainties in lateral buckling control [58]. Eton [4] proposed the anchoring point as shown in Fig. 46 of which pipeline is not allowed to move, in this case, the points can be mitigated with the EK process. Typically short pipeline [2] with length between 2-5km are usually being affected by pipeline walking. The current subsea capabilities such as the umbilical cable may be used for power supply and control. Due to the high saline environment, high power consumption will serve as disadvantage using the EK method. However, Eton [4] suggested that consolidation of small volume of the soil during axial displacement of pipeline is needed to significantly increase its resistance. This implies that lower power may be required than expected.

5 Conclusion

This study shows the capabilities of ABAQUS tool for electro-osmotic consolidation analyses. Applied voltage have been the main driven force in the EK process and the time of treatment also plays an important role on the soil settlement. From the obtained results, it is shown that the lower voltage can be compensated with longer treatment time of the soil. The larger settlement occurs beside and below the pipe invert surfaces due to electrical field influence within these regions. The resultant effect of pore water pressure dissipation from the soil void led to the increase in the soil effective stress. A comparisons between the EK and non-EK process, the force required to displace the pipeline in vertical, axial and lateral direction indicates significant increase.

5.1 Further Studies

Some areas that requires further studies to have better understanding of the EK effect on the pipe-soil interaction behaviours are stated below:

- considerations to cyclic loading, to determine if higher shearing rate may cause additional pore pressure and cancel out the hardening effect as suggested by [3]. It is not clear what the effect of this cyclic movement would be on the Electro-kinetic modified soil.
- Studies with other velocities and other stress conditions under pipe as pipeline displaces with varying velocities and loading conditions.
- Investigation on the numbers of electrode/electrode configurations, merit further research to have clarity on the optimum numbers of electrodes to minimise complexity and save cost.
- Consideration on the effect of polarity reversal and intermittent voltage application on soil settlement.

Acknowledgments

The authors wish to appreciate the support and funding provided by the Petroleum Technology Development Fund (PTDF) Nigeria.

References

- [1] J.C. Ballard, C. De Brier, K. Stassen, R. a Jewell, Observations of pipe-soil response from in-situ measurements, in: Proc. Offshore Technol. Conf., Offshore Technology Conference, Houston, Texas, 2013: pp. 6–9. doi:10.4043/24154-MS.
- [2] D. Bruton, M. Bolton, M. Carr, D. White, Pipe-Soil Interaction during Lateral Buckling and Pipeline Walking — The SAFEBUCK JIP, in: Proc. Offshore Technol. Conf., Offshore Technology Conference, Houston, Texas, 2008: p. 20pp. doi:10.4043/19589-MS.
- [3] D.J. White, M.E. Campbell, N.P. Boylan, M.F. Bransby, A New Framework For Axial Pipe-Soil Interaction, Illustrated By Shear Box Tests On Carbonate Soils, in: Proc. 7th Int. Conf. Offshore Site Investig. Geotech., Society of Underwater Technology, London, 2012: pp. 379–387.
- [4] G.E. Eton, Mitigation against lateral buckling and axial walking of subsea pipeline, Doctor of Philosophy thesis, Institute of Resilient Infrastructure, School of Civil Engineering, University of Leeds, 2011.
- [5] A.Z. Al-Hamdan, K.R. Reddy, Electrokinetic Remediation Modeling Incorporating Geochemical Effects, *J. Geotech. Geoenvironmental Eng.* 134 (2008) 91–105. doi:10.1061/(ASCE)1090-0241(2008)134:1(91).
- [6] C. Jones, S. Glendinning, Soil consolidation and strengthening using electrokinetic geosynthetics—concepts and analysis, *Geosynthetics*. (2006) 411–414. [http://www.electrokinetic.co.uk/Downloads/E5 Soil Consolidation and strengthening with EKG.pdf](http://www.electrokinetic.co.uk/Downloads/E5%20Soil%20Consolidation%20and%20strengthening%20with%20EKG.pdf).
- [7] J. Virkutyte, M. Sillanpaa, P. Latostenmaa, Electrokinetic soil remediation - Critical overview, *Sci. Total Environ.* 289 (2002) 97–121. doi:10.1016/S0048-9697(01)01027-0.
- [8] J.K. Mitchell, K. Soga, *Soil Composition and Engineering Properties*, 3rd ed., John Wiley & Sons, 2005. http://www.knovel.com/web/portal/browse/display?_EXT_KNOVEL_DISPLAY_bookid=1736&VerticalID=0.
- [9] H. Wu, W. Wu, L. Hu, Numerical model of electro-osmotic consolidation in clay, *Géotechnique*. 62 (2012) 537–541. doi:10.1680/geot.11.T.008.
- [10] K.Y. Lo, S. Micic, J.Q. Shang, Y.N. Lee, S.W. Lee, Electrokinetic strengthening of a marine sediment using intermittent current, *Can. Geotech. J.* 38 (2001) 287–302. doi:10.1139/cgj-38-2-287.
- [11] J. Staff, In-Situ Casing Consolidation by Electrokinetic Methods, *Pet. Technol.* 50 (1998) 51–53. doi:10.2118/0298-0051-JPT.
- [12] S. Micic, J.Q. Shang, K.Y. Lo, Electrocementation of a marine clay induced by electrokinetics, *Int. J. Offshore Polar Eng.* 13 (2003) 308–315.
- [13] L. HU, H. WU, Mathematical model of electro-osmotic consolidation for soft ground improvement, *Géotechnique*. 64 (2014) 155–164. doi:10.1680/geot.13.P.096.
- [14] L. Bjerrum, J. Mowm, O. Eide, Application of Electro-Osmosis to a Foundation Problem in a Norwegian Quick Clay, *Géotechnique*. 17 (1967) 214–235. doi:10.1680/geot.1967.17.3.214.
- [15] J. Yuan, M. a Hicks, C. Jommi, Large strain consolidation of clays : Numerical comparison between evaporation and electro-osmosis dewatering, *Comput. Methods Recent Adv. Geomech.* (2015) 1655–1660.
- [16] J. Yuan, M.A. Hicks, Numerical analysis of electro-osmosis consolidation: a case study, *Géotechnique Lett.* 5 (2015) 147–152. doi:10.1680/geolett.15.00045.
- [17] F. Burnotte, G. Lefebvre, G. Grondin, A case record of electroosmotic consolidation of soft clay with improved soil–electrode contact., *Can. Geotech. J.* 41 (2004) 1038–1053. doi:10.1139/t04-045.
- [18] M. Esrig, Pore pressures, consolidation, and electrokinetics, *J. Soil Mech. Found. Div.* Vol 94 (1968) 899–921.
- [19] C. Lewis, WR and Humpheson, Numerical analysis of electroosmotic flow in soils, *J. Soil Mech. Found. Div. ASCE*. Vol 95 (1973) 603–616.
- [20] J. Wan, T and Mitchell, Electro-osmotic consolidation of soils, *J. Soil Mech. Found. Div. ASCE*. Vol 102, (1976) 473–491.
- [21] J.K. Mitchell, Components of Pore Water Pressure and Their Engineering Significance, *Clays Clay Miner.* 9 (1960) 162–184. doi:10.1346/CCMN.1960.0090109.
- [22] K.Y. Lo, S. Micic, J.Q. Shang, Electrokinetic Strengthening of Soft Marine Clays, in: Proc. Ninth Int. Offshore Polar Eng. Conf., International Society of Offshore and Polar Engineers, Brest, France, 1999: pp. 1–6.
- [23] S. Micic, J.Q. Shang, K.Y. Lo, Electrokinetic strengthening of marine clay adjacent to offshore foundations, *Int. J. Offshore Polar Eng.* 12 (2002) 64–73.
- [24] S. Micic, K.Y. Lo, J.Q. Shang, Increasing load-carrying capacities of offshore foundations in soft clays, *J. Pet. Technol.* 56 (2004) 53–55.
- [25] R. Merifield, D.J. White, M.F. Randolph, The ultimate undrained resistance of partially embedded pipelines, *Géotechnique*. 58 (2008) 461–470. doi:10.1680/geot.2007.00097.
- [26] C.P. Aubeny, H. Shi, J.D. Murff, Collapse Loads for a Cylinder Embedded in Trench in Cohesive Soil, *Int. J. Geomech.* 5 (2005) 320–325. doi:10.1061/(ASCE)1532-3641(2005)5:4(320).
- [27] R.S. Merifield, D.J. White, M.F. Randolph, Effect of Surface Heave on Response of Partially Embedded Pipelines on Clay, *J. Geotech. Geoenvironmental Eng.* 135 (2009) 819–829. doi:10.1061/(ASCE)GT.1943-5606.0000070.
- [28] S. Muthukrishnan, J. Kodikara, P. Rajeev, Numerical modelling of undrained vertical load- displacement behaviour of

- offshore pipeline using coupled analysis, in: 2011 Pan-Am CGS Geotech. Conf., 2011: pp. 1–8.
- [29] M.F. Randolph, D.J. White, Pipeline Embedment in Deep Water: Processes and Quantitative Assessment, in: Proc. Offshore Technol. Conf., Offshore Technology Conference, Houston, Texas, 2008: pp. 1–16. doi:10.4043/19128-MS.
- [30] J. Ballard, H. Falepin, Towards more advanced pipe-soil interaction models in finite element pipeline analysis, in: Proc. SUT Annu. Conf., Society of Underwater Technology, Perth, Western Australia, 2009: pp. 1–5.
- [31] Z.J. Westgate, M.F. Randolph, D.J. White, S. Li, The influence of sea state on as-laid pipeline embedment: A case study, *Appl. Ocean Res.* 32 (2010) 321–331. doi:10.1016/j.apor.2009.12.004.
- [32] J. Oliphant, A. Maconochie, Axial Pipeline-Soil Interaction, in: Int. Soc. Offshore Polar Eng., International Society of Offshore and Polar Engineers, San Francisco, California, USA, 2006: pp. 100–107.
- [33] F. Casola, A. El-chayeb, S. Greco, A. Carlucci, Characterization of Pipe Soil Interaction and Influence on HPHT Pipeline Design, *Int. Soc. Offshore Polar Eng.* 8 (2011) 111–121.
- [34] M.F. Randolph, A.R. House, The complementary roles of physical and computational modelling, *Int. J. Phys. Model. Geotech.* 1 (2001) 1–8.
- [35] E.J. Hansen, V.E. Saouma, Numerical simulation of reinforced concrete deterioration: Part II—steel corrosion and concrete cracking, *ACI Mater. J.* 96 (1999) 331–338.
- [36] Dassault Systèmes, Abaqus analysis user guide, 2012.
- [37] Y. Ansari, G.P. Kouretzis, D. Sheng, An effective stress analysis of partially embedded offshore pipelines: Vertical penetration and axial walking, *Comput. Geotech.* 58 (2014) 69–80. doi:10.1016/j.compgeo.2014.01.011.
- [38] Vermeer, A. P., A. Verruijt, An Accuracy Condition for Consolidation by Finite Elements, *Int. J. Numer. Anal. Methods Geomech.* 5 (1981) 1–14. doi:10.1002/nag.1610050103.
- [39] K. Krost, D.J. White, S.M. Gourvenec, Consolidation around partially embedded seabed pipelines, *Géotechnique*. 61 (2011) 167–173. doi:10.1680/geot.8.T.015.
- [40] S.M. Gourvenec, D.J. White, Elastic Solutions for Consolidation Around Seabed Pipelines, in: Otc, 2010: pp. 3–6. doi:10.4043/20554-MS.
- [41] A. Rittirong, J.Q. Shang, Numerical analysis for electro-osmotic consolidation in two-dimensional electric field, *Eighteenth Int. Offshore Polar Eng. Conf.* 8 (2008) 566–572.
- [42] E. Mohamedelhasan, J.Q. Shang, Effects of electrode materials and current intermittence in electro-osmosis, *Proc. Inst. Civ. Eng. - Gr. Improv.* 5 (2001) 3–11. doi:10.1680/grim.2001.5.1.3.
- [43] L. Xie, C. Shang, Effects of copper and palladium on the reduction of bromate by Fe(0), *Chemosphere*. 64 (2006) 919–930. doi:10.1016/j.chemosphere.2006.01.042.
- [44] D.T. Bergado, I. Sasanakul, S. Horpibulsuk, Electro-osmotic consolidation of soft Bangkok clay using copper and carbon electrodes with PVD, *Geotech. Test. J.* 26 (2003) 277–288. doi:10.1520/GTJ11309J.
- [45] H.R.C. Dingle, D.J. White, C. Gaudin, Mechanisms of pipe embedment and lateral breakout on soft clay, *Can. Geotech. J.* 45 (2008) 636–652. doi:10.1139/T08-009.
- [46] W.D. Callister, D.G. Rethwisch, *Materials science and engineering : an introduction*, 9th ed., John Wiley & Sons, 2014.
- [47] Engineering tool box, Conductivity of some common materials and gases, http://www.engineeringtoolbox.com/thermal-Conductivity-d_429.html. (2015). http://www.engineeringtoolbox.com/thermal-conductivity-d_429.html (accessed March 2, 2015).
- [48] D. Carneiro, A. Castelo, Walking analyses of HP/HT pipelines with sliding end structures using different FE models, in: Rio Pipeline 2011, Rio Pipeline Conference & Exposition, Rio de Janeiro, Brazil, 2011: pp. 1–11.
- [49] M. Carr, F. Sinclair, D. Bruton, Pipeline Walking--Understanding the Field Layout Challenges and Analytical Solutions Developed for the Safebuck JIP, *SPE Proj. Facil. Constr.* 3 (2008) 1–9. doi:10.2118/120022-PA.
- [50] P. Cormie, J.M. McBride, G.O. McCaulley, A. Jensen, E. Lidell, The Influence of C Onscience, *J. Strength Cond. Res.* 16 (2009) 1042–1049. doi:10.1519/R-21636.1.
- [51] Q. Bai, Y. Bai, Lateral Buckling and Pipeline Walking, in: *Subsea Pipeline Des. Anal. Install.*, 2014: pp. 221–253. doi:10.1016/B978-0-12-386888-6.00010-9.
- [52] D. Bruton, D.J. White, C.Y. Cheuk, “Pipe/soil interaction behavior during lateral buckling, including large-amplitude cyclic displacement tests by the safebuck JIP,” in: *Offshore Technol. Conf.*, 2006: pp. 1–10. doi:10.4043/17944-MS.
- [53] A. Altaee, B.H. Fellenius, Finite Element Modeling of Lateral Pipeline-Soil Interaction, in: 114th Int. Conf. Offshore Mech. Arct. Eng. OMAE 96, Florence, Italy, 1996: pp. 283–300.
- [54] T.D. O’Rourke, C.H. Trautmann, Lateral force-displacement of buried pipe response, *J. Geotech. Eng.* 111 (1985) 1077–1092. doi:10.1061/(ASCE)1080-9009(1985)111:10<1077::AID-JGEO1077>2.0.CO;2.
- [55] V.B. Smith, D.J. White, OTC-24856-MS Volumetric Hardening in Axial Pipe Soil Interaction, in: *Offshore Technol. Conf. - ASIA*, Offshore Technology Conference, Kuala Lumpur, Malaysia, 2014: pp. 1–11. doi:10.4043/24856-MS.
- [56] V. Smith, A.M. Kaynia, Pipe-soil interaction under rapid axial loading, *Front. Offshore Geotech.* III. (2015) 978–1.
- [57] D. Perinet, J. Simon, Lateral Buckling and Pipeline Walking Mitigation in Deep Water, *Offshore Technol. Conf.* (2011) 2–5.

doi:10.4043/21803-MS.

- [58] H. Rong, R. Inglis, G. Bell, Z. Huang, R. Chan, J.P. Kenny, Evaluation and Mitigation of Axial Walking with a Focus on Deep Water Flowlines, in: Proc. Offshore Technol. Conf., Houston, TX, OTC 19862, Offshore Technology Conference, Houston, Texas, 2009: pp. 1–10.